Astron. Astrophys. 352, 85–102 (1999)

ASTRONOMY AND ASTROPHYSICS

Optical imaging of the host galaxies of X-ray selected BL Lacertae objects⋆

Renato Falomo[1] **and Jari K. Kotilainen**[2]

[1] Osservatorio Astronomico di Padova, Vicolo dell'Osservatorio 5, 35122 Padova, Italy (falomo@pd.astro.it)
[2] Tuorla Observatory, University of Turku, Väisäläntie 20, 21500 Piikkiö, Finland (jkotilai@stardust.astro.utu.fi)

Received 21 July 1999 / Accepted 29 September 1999

Abstract. We investigate the properties of the host galaxies of X–ray selected (high frequency peaked) BL Lac objects using a large and homogeneous data set of high spatial resolution R–band observations of 52 BL Lacs in the EMSS and Slew samples. The redshift distribution of the BL Lacs ranges from z = 0.04 to z>0.7, with average and median redshifts z = 0.26 and z = 0.24, respectively. Eight objects are at unknown redshift.

We are able to resolve 45 objects out of the 52 BL Lacs. For all the well resolved sources, we find the host to be a luminous elliptical galaxy. In a few cases a disk is not ruled out but an elliptical model is still preferred.

The average absolute magnitude of the host galaxies is $\langle M_R(host)\rangle$ = $-$23.9±0.6, while the average scale length of the host is ⟨R(e)⟩ = 9±5 kpc. There is no difference in the host properties between the EMSS and Slew samples. We find a good agreement between the results derived by the surveys of Wurtz et al. (ground-based data) and Urry et al. (HST data), and by our new deeper imaging. The average luminosity of the BL Lac hosts is between those of F-R I and F-R II radio galaxies in Govoni et al., supporting the idea that both radio galaxy types could contribute to the parent population. The BL Lac hosts follow the F-P relation for giant ellipticals and exhibit a modest luminosity evolution with redshift. Finally, we find a slight correlation between the nuclear and host luminosity and a bimodal distribution in the nuclear/host luminosity ratio.

Key words: galaxies: active – galaxies: BL Lacertae objects: general – galaxies: interactions – galaxies: nuclei – galaxies: photometry – galaxies: structure

1. Introduction

BL Lacertae objects are the most extreme class of active galactic nuclei (AGN), exhibiting strong, rapidly variable polarization and continuum emission, and core-dominated radio emission with apparent superluminal motion (see e.g. Kollgaard et al. 1992 for references). These properties have led to the commonly accepted view that BL Lacs are dominated by Doppler-boosted synchrotron emission from a relativistic jet nearly along our line-of-sight (Blandford & Rees 1978). The line emission of BL Lacs is absent or weak, making their redshift determination rather difficult.

In the current unified models of radio-loud AGN (e.g. Urry & Padovani 1995), BL Lacs are identified as low luminosity, core-dominated F-R I (Fanaroff & Riley 1974) radio galaxies (RG) viewed nearly along the axis of the relativistically boosted jet. This model appears supported by the comparison of their extended radio luminosity and morphology (e.g. Perlman & Stocke 1993), host galaxy luminosity and morphology (e.g. Wurtz et al. 1996; hereafter WSY96) and space density and beamed luminosity functions (e.g. Padovani & Urry 1990; Morris et al. 1991; Celotti et al. 1993).

Knowledge of the properties of the host galaxies and environments where AGN live is fundamental for the understanding of the formation of AGN in galaxies. Comparison of orientation-independent properties of BL Lacs, such as the host galaxies and environment, with those of RGs, allow one to test the unified model based on orientation (Antonucci 1993; Urry & Padovani 1995). The frequency of close companions will determine whether interactions are important for triggering of the BL Lac activity, as seems to be the case for quasars (e.g. Heckman 1990; Hutchings & Neff 1992). Possible cosmological evolution in the properties of the hosts and environments can be studied by comparing AGN properties at different redshifts. Finally, the alternative gravitational lensing hypothesis for BL Lac activity (Ostriker & Vietri 1990) can be tested by measuring the predicted offsets between the BL Lacs and their host galaxies.

Recent studies of BL Lac hosts and close environments from the ground and with the HST (see Pesce et al. 1995; Falomo 1996; Owen et al. 1996; WSY96; Wurtz et al. 1997; Falomo et al. 1997; Scarpa et al. 1999a; Urry et al. 1999a; Urry et al. 1999b, hereafter U99b; Heidt et al. 1999) have shown that their host galaxies are luminous ($M_R \sim -23$ to -24) and large (R(e) = 10±7 kpc) elliptical galaxies. They are on average ∼1 mag brighter than L* galaxies (e.g. Mobasher et al. 1993) and of similar luminosity or slightly fainter than the brightest cluster galaxies (BCG; e.g. Hoessel et al. 1980). Intriguingly, BL Lac hosts appear slightly fainter than F-R I hosts and resemble better

Send offprint requests to: R. Falomo

⋆ Based on observations made with the Nordic Optical Telescope, operated on the island of La Palma, jointly by Denmark, Finland, Iceland, Norway and Sweden, in the Spanish Observatorio del Roque de los Muchachos of the Instituto de Astrofisica de Canarias.

typical F-R II hosts. Detections or claims of disk hosts and/or inner disks components have been made in a handful of sources (e.g. MS 0205.7+3509 Stocke et al. 1995; OQ 530 Abraham et al. 1991; PKS 1413+135, McHardy et al. 1991; PKS 0548-322, Falomo et al. 1995; 1ES 1959+650, Heidt et al. 1999;). While it is not unreasonable to find small inner disk structures similarly to what found in normal ellipticals, the objects with a disk dominated host galaxy are rather controversial (for details see: Falomo et al. 1997; Stocke et al. 1992; Lamer et al. 1999; Scarpa et al. 1999a,b).

Close companions have been found around many BL Lacs, some with signs of interaction, but the physical association has been confirmed only in some cases through spectroscopic measurements. BL Lacs usually reside in poor clusters, unlike F-R I RGs. A modified unified model has therefore been proposed in which BL Lacs either include partly F-R IIs in addition to F-R Is, or BL Lacs avoid the brightest F-R Is and the F-R Is in rich clusters at low redshift (WSY96). This scenario seems also supported by recent measurements of radio polarization of BL Lacs (Stanghellini et al. 1997) that show signature of a F-R II population.

Similarly to the case of quasars (e.g. Hutchings et al. 1994; Rönnback et al. 1996; Bahcall et al. 1997), the study of BL Lac host galaxies is rather problematic because of the presence of the bright nucleus that swamps the light of the host galaxy, although the nucleus/host luminosity ratio of the BL Lacs is smaller than that of quasars. The use of HST images can substantially improve the ability to study the host close to the nucleus, however, as we shall show in Sect. 4.2.2, HST data are usually not deep enough to properly investigate the external fainter regions of the host galaxies (see also e.g. Hutchings et al. 1994; Bahcall et al. 1997).

In this paper we report on a large, homogeneous data set of observations of BL Lacs secured mainly with sub-arcsec resolution from the Nordic Optical Telescope (NOT) in La Palma. We have observed the complete sample of 26 X-ray selected (or high frequency peaked, HBL) BL Lacs derived from the *Einstein* Medium Sensitivity Survey (EMSS; Stocke et al. 1991). This sample is almost complete for multiwavelength information and redshift (although some redshifts are tentative and probably wrong, see the Appendix) and most of the objects are at z$<$0.3, ensuring the detection of the host in most cases with reasonable observing time. Additionally, we obtained images for 26 BL Lacs in the *Einstein* Slew Survey (Perlman et al. 1996). These BL Lacs are also of HBL type and are compared with the EMSS targets. Based on the current data, we have previously published a separate study of the peculiar BL Lac object MS 0205.7+3509 (Falomo et al. 1997).

The structure of this paper is as follows: In Sect. 2 we describe the samples of the objects observed. In Sect. 3 we give details of the observations, data reduction and describe the image analysis. Results and discussion on the overall properties of the host galaxies, including comparison with previous studies of BL Lacs and other types of AGN are given in Sect. 4. The main conclusions from this study are summarized in Sect. 5. In the Appendix, we give comments for individual objects. Throughout this paper, H_0 = 50 km s^{-1} kpc^{-1} and $q_0 = 0$ are adopted.

2. The samples

2.1. The EMSS sample

The EMSS survey (Gioia et al. 1990; Morris et al. 1991; Stocke et al. 1991; Maccacaro et al. 1994) is a flux–limited complete sample of faint X–ray sources discovered serendipitously in numerous *Einstein* Imaging Proportional Counter (IPC) fields centered on high galactic latitude ($b > 20\,\deg$) targets. It covers 780 $\deg^2$ in the 0.3–3.5 keV soft X–ray band with limiting sensitivity ranging from $\sim 5 \times 10^{-14}$ to $\sim 3 \times 10^{-12}$ erg cm^{-2} s^{-1}. The EMSS includes 34 BL Lac objects and 4 BL Lac candidates (as listed in Padovani & Giommi 1995), selected to have the observed equivalent width of any emission line EW $<$5 Å. Moreover, if a Ca II H+K break is present due to starlight in the BL Lac host galaxy, its contrast must be $\leq 25\,\%$, much less than for a typical giant non-active elliptical galaxy ($\sim$50%).

2.2. The Slew survey sample

The IPC Slew survey (Perlman et al. 1996) was constructed using the *Einstein* slew data taken when the satellite was moving from one target to the next (Elvis et al. 1992) and covers a large fraction of the sky with limiting sensitivity ranging from $\sim 5 \times 10^{-12}$ to $\leq 1 \times 10^{-12}$ erg cm^{-2} s^{-1} in the 0.3–3.5 keV soft X–ray band. Padovani & Giommi (1995) list a total of 60 Slew BL Lacs and 9 BL Lac candidates extracted from the Slew survey adopting the same classification criteria as for the EMSS survey.

2.3. Our selection criteria

The observed BL Lacs were selected from the EMSS and Slew samples to have declination $\delta \geq$–15 deg, to be observable at the NOT. This limit excluded five BL Lacs and three BL Lac candidates of the EMSS sample. Of the remaining 29 BL Lacs and one BL Lac candidate, 28 (93%) were observed at the NOT, the only exceptions being MS 1019.0+5139 and MS 1207.9+3945.

In the Slew sample, seven BL Lacs and two BL Lac candidates do not satisfy our declination limit. Furthermore, of the remaining 53 BL Lacs and 7 candidates, 14 are of low frequency peak (LBL) type while 4 belong also to the EMSS sample. Of the final sample of 35 Slew BL Lacs and 7 Slew BL Lac candidates, 26 (62%) were observed at the NOT. The selection of the Slew objects observed was based only on observability conditions. General properties of the observed BL Lacs are given in Table 1, Columns (1)–(7), where Column (1) gives the name of the object, Column (2) the redshift, Column (3) the apparent V–band magnitude, Columns (4) and (5) the 5 GHz and 2 keV flux densities, respectively, and Columns (6) and (7) the optical–X-ray and radio–optical spectral indices, respectively.

The redshift distribution of the observed objects from EMSS and Slew is shown in Fig. 1. The average redshifts of the BL Lacs with known redshift in the samples are: 0.319$\pm$0.133 (EMSS, all); 0.314$\pm$0.120 (EMSS, observed); 0.201$\pm$0.124 (Slew, all)

Table 1. General properties of the BL Lacs and journal of the observations.

Name	z	V	S(5 GHz) (mJy)	S(2 keV) (μJy)	α(O–X)	α(R–O)	Date	T(int) (sec)	Sky (mag)	Seeing ($''$)	A(r) (mag)
1ES 0033+595	...	19.5	66.0	2.22	0.45	0.61	21/09/98	600	21.0	0.64	1.94
1ES 0120+340	0.272	15.2	33.6	1.86	1.06	0.28	23/12/95	1200	19.72	0.51	0.24
MS 0122.1+0903	0.339	20.0	1.4	0.15	0.91	0.34	22/09/98	1800	21.01	0.58	0.20
MS 0158.5+0019	0.229:	18.0	11.3	0.67	0.88	0.36	22/09/98	3600	20.9	0.63	0.12
MS 0205.7+3509	0.318:	19.2	3.6	0.11	1.08	0.36	23/12/95	2400	19.97	0.68	0.29
1ES 0229+200	0.139	14.7	49.1	1.13	1.22	0.27	22/09/98	2400	21.01	0.60	0.41
MS 0257.9+3429	0.247	18.5	10.0	0.25	1.02	0.40	23/12/95	1800	20.95	0.53	0.41
MS 0317.0+1834	0.190	18.1	17.0	2.56	0.71	0.41	24/12/95	1800	20.88	0.62	0.46
1ES 0347-121	0.188	18.2	9.0	2.32	0.64	0.36	23/09/98	1800	21.01	1.12	0.17
1ES 0414+009	0.287	17.5	70.0	3.64	0.67	0.47	24/02/98	2400	20.2	0.87	0.41
MS 0419.3+1943	0.512:	20.3	8.0	0.53	0.62	0.50	24/12/95	3600	19.9	0.73	0.84
1ES 0446+449	0.203:	18.5	139.4	0.63	0.81	0.60	24/12/95	1800	20.79	0.59	2.52
1ES 0502+675	0.341	17.0	32.7	1.36	0.92	0.37	21/09/98	3600	21.01	0.78	0.53
1ES 0525+713	0.249:	19.0	9.0	0.80	0.69	0.42	21/09/98	1200	20.9	0.68	0.41
MS 0607.9+7108	0.267	19.6	18.2	0.27	0.86	0.52	24/12/95	3300	20.67	0.67	0.41
1ES 0647+250	...	15.8	73.4	2.36	1.01	0.35	21/09/98	900	20.9	0.65	0.65
MS 0737.9+7441	0.315	16.9	24.0	0.46	1.10	0.40	24/12/95	1500	20.68	0.77	0.17
1ES 0806+524	0.136:	15.0	171.9	1.38	1.22	0.36	24/02/98	3000	20.73	0.96	0.20
MS 0922.9+7459	0.638:	19.7	3.3	0.22	0.90	0.39	24/12/95	3600	20.66	0.71	0.12
1ES 0927+500	0.188	17.2	18.3	0.67	1.00	0.34	24/12/95	2100	20.84	0.93	0.08
MS 0950.9+4929	$>$0.5	19.3	3.3	0.21	0.88	0.36	02/06/95	1320	20.26	0.83	0.05
MS 0958.9+2102	0.334	19.8	1.5	0.04	1.16	0.34	02/06/95	1320	19.88	0.88	0.12
1ES 1011+496	0.210	16.1	286.0	0.54	1.21	0.48	24/02/98	2400	20.75	1.66	0.05
1ES 1028+511	0.239:	16.6	44.2	1.88	0.92	0.37	24/12/95	1500	20.96	0.57	0.05
1ES 1106+244	...	18.7	18.1	0.56	0.80	0.45	25/02/98	2400	20.75	2.02	0.05
1ES 1118+424	0.124:	17.0	35.0	1.41	0.91	0.38	24/12/95	1200	21.04	0.60	0.10
1ES 1212+078	0.130	16.0	94.0	0.27	1.25	0.43	25/02/98	2400	20.23	1.53	0.08
1ES 1218+304	0.182:	16.4	56.0	2.51	0.90	0.37	25/02/98	2400	20.39	0.98	0.08
MS 1221.8+2452	0.218:	17.6	26.4	0.26	1.20	0.41	31/05/95	1200	19.95	1.14	0.10
MS 1229.2+6430	0.164	16.9	42.0	0.70	1.15	0.39	01/06/95	1200	20.83	0.59	0.10
MS 1235.4+6315	0.297	18.6	7.0	0.39	0.99	0.37	01/06/95	1200	20.78	0.70	0.08
1ES 1255+244	0.141	15.4	7.4	3.66	1.30	0.17	24/12/95	900	20.36	0.58	0.08
MS 1256.3+0151	...	20.0	8.0	0.05	1.11	0.49	31/05/95	1200	19.41	1.34	0.08
MS 1402.3+0416	0.344:	17.1	20.8	0.10	1.33	0.34	03/06/95	1920	20.6	0.84	0.10
MS 1407.9+5954	0.495	19.7	16.5	0.41	0.81	0.52	31/05/95	1800	19.69	1.36	0.08
MS 1443.5+6349	0.299	19.6	11.6	0.33	0.85	0.49	02/06/95	1920	20.82	0.76	0.08
MS 1458.8+2249	0.235:	16.8	29.8	0.22	1.35	0.36	02/06/95	1320	20.97	0.64	0.17
1ES 1517+656	$>$0.7	15.9	39.0	1.19	1.11	0.30	21/09/98	2400	19.5	0.70	0.10
MS 1534.2+0148	0.312	18.7	34.0	0.43	0.94	0.51	01/06/95	1920	20.41	0.65	0.24
MS 1552.1+2020	0.222	17.7	37.5	0.89	0.97	0.44	02/06/95	2100	20.88	0.65	0.17
MS 1704.9+6046	0.280	19.1	1.8	0.10	1.13	0.30	31/05/95	1800	19.31	1.95	0.10
MS 1757.7+7034	0.407	18.3	7.2	0.48	0.98	0.35	24/09/98	2400	20.9	1.20	0.20
1ES 1853+671	0.212	16.4	12.1	0.28	1.19	0.28	21/09/98	2400	21.01	0.64	0.26
1ES 1959+650	0.048:	13.7	251.6	3.64	1.19	0.32	23/09/98	1800	20.99	0.62	0.48
1ES 2037+521	0.05?	19.0	32.5				22/09/98	2400	20.91	0.77	2.21
MS 2143.4+0704	0.237	18.0	50.0	0.46	1.03	0.49	01/06/95	1320	20.57	0.82	0.22
1ES 2321+419	0.059:	17.0	19.0	0.27	1.19	0.32	24/09/98	1200	21.14	0.69	0.44
1ES 2326+174	0.213	16.8	18.4	0.56	1.02	0.35	21/09/98	1800	20.9	0.70	0.17
MS 2336.5+0517	...	20.3	4.9	0.10	0.93	0.47	24/12/95	3600	18.84	0.61	0.26
1ES 2343-151	0.226	19.2	8.2	0.30	0.83	0.42	23/09/98	3000	20.9	0.85	0.10
1ES 2344+514	0.044	15.5	215.2	1.14	1.18	0.41	22/09/98	1200	20.9	0.99	0.74
MS 2347.4+1924	0.515	20.8	3.2	0.10	0.86	0.47	23/09/98	1800	20.9	0.65	0.20

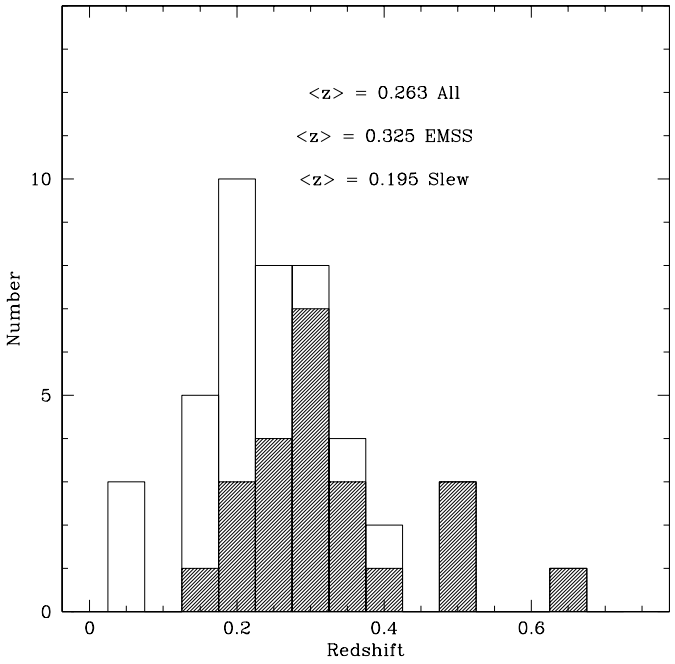

Fig. 1. Redshift distribution of the observed BL Lac objects. Hatched area show EMSS objects

Table 2. Description of the observing runs.

Date	Instrument/CCD	″/px	Photometry
31/5-3/6/95	BroCam/Tk1024A	0.176	good
20-23/12/95	BroCam/Tk1024A	0.176	No (20-22/12)
			Yes (23/12)
24-26/2/98	HiRAC/Loral	0.11	poor
21-24/9/98	HiRAC/Loral	0.11	good

and 0.190±0.091 (Slew, observed). It can be seen that a) the observed and full samples do not differ significantly in their redshift distribution and b) the Slew survey tends to select BL Lacs at somewhat lower redshift than the EMSS survey because of the brighter X-ray flux limit of the Slew survey.

3. Observations, data reduction and analysis

Optical images were obtained during four observing runs using the 2.5m NOT telescope at La Palma. We used the BroCam camera (1024^2 px, $0\farcs176$ px^{-1}) for observations in 1995 while the HiRAC camera (2048^2 px, $0\farcs11$ px^{-1}) was used for observations in 1998 (for details, see Table 2). In all observations the Cousins R filter was used to image the objects. The observations were performed mostly during photometric conditions and photometric calibration of each night was obtained from frequent observations of Landolt (1992) standard stars. Some objects were imaged during non photometric conditions, therefore we secured additional short exposure images of these targets during photometric nights to calibrate these frames using reference stars. Seeing conditions were generally very good with average and median seeing FWHM = $0\farcs84$ and $0\farcs70$, respectively.

In most cases both a short (typically 2 minutes) and a long (ranging from 10 to 60 minutes, average 20 minutes) integration were obtained. The short and long exposures were then combined to form an image of the target well exposed in the external (fainter) regions while avoiding saturation of the bright nucleus. In some cases where the nucleus was much brighter than the surrounding nebulosity, several intermediate length integrations were combined in order to obtain a final well exposed image. Moreover, the combination of multiple images allowed for identifying and removing cosmic ray hits.

In Table 1, Columns (8)–(12), we give a journal of the observations with details for each object. Column (8) gives the date of observation, Columns (9) and (10) report the total exposure time and the sky brightness, while in Columns (11) and (12) the seeing FWHM measured from stellar images and the Galactic extinction used are given.

Data reduction was performed following standard procedures (including bias subtraction, flat fielding and cosmic ray rejection) available in IRAF[1]. The level of the sky was derived sampling several regions over the image and checking for residual gradients in the background level. Since no significant gradient was found a single flux level for the sky was used. From these final images we have extracted for each object the azimuthally averaged radial brightness profile down to a surface brightness $\mu_R \sim 26$ mag arcsec^{-2}. Any obvious extra features (e.g. companions and foreground stars) were removed (masked) from the image in order to avoid contamination of the radial profile. In order to derive the shape of the point spread function (PSF), we have similarly extracted the radial profile of a large number of stars in each field. Since the field of view of our images is sufficiently large, this was always easily obtained using the object frame. Many stellar profiles were combined in order to obtain a good PSF both in the core and in the wings.

Subsequent analysis consisted in comparing each profile of the BL Lac object with its PSF and, for the resolved sources, fitting the observed luminosity profile with a model. We used the simple approach of assuming the observed object is composed of a nuclear (unresolved) source, described by a PSF, plus a galaxy, modeled by either a de Vaucouleurs (μ(r) $\propto$ r$^{0.25}$) or an exponential disk (μ(r) $\propto$ r), convolved with the proper PSF. More complex models, for example a generalized de Vaucouleurs law (e.g. the Sersic law $\mu \propto r^{1/n}$), increases the number of free parameters and do not offer real advantages for the characterization of the host galaxies.

From the best fit of the profiles we have determined the parameters of the host galaxy (μ_o, r$_e$, total magnitude) as well as the magnitude of the nuclear source. These parameters are reported in Table 3, Columns (1)–(7), where Column (1) gives the name of the object, Column (2) its redshift, Columns (3) and (4) the central surface brightness of bulge component and its scale length, Columns (5)–(6) the apparent magnitude of the

[1] IRAF is distributed by the National Optical Astronomy Observatories, which are operated by the Association of Universities for Research in Astronomy, Inc., under cooperative agreement with the National Science Foundation

nuclear and galactic components, and Column (7) the reduced χ^2 of the best fit. Absolute quantities were derived after applying correction for Galactic extinction and redshift (K-correction). The former was determined using the Bell Lab Survey of neutral hydrogen N_H converted to E_{B-V} (Stark et al. 1992; Shull & Van Steenberg 1985), while the latter was computed from the model of Coleman et al. (1980) for elliptical galaxies.

4. Results and discussion

4.1. Absolute magnitude and scale length

In Fig. 2 we report for each object the radial luminosity profile together with its best-fit decomposition into nucleus and host galaxy components. We are able to resolve 45 objects out of the 52 observed sources. For almost all of the clearly resolved sources we are able to fit the luminosity profile of the host galaxy with an elliptical model while a disk model gave a significantly worse fit. For a few distant and marginally resolved sources (see Table 3 and Fig. 2), we cannot rule out a disk model but even in these cases an elliptical model is a good representation of the host galaxy.

The absolute magnitudes of the nucleus and the host galaxies are reported in Table 3, Columns (8)–(12), where Column (8) gives the applied K–correction, Columns (9) and (10) the absolute magnitudes of the nuclear component and the host galaxy, and Columns (11) and (12) the scale length and surface brightness at the effective radius. The distributions of the host galaxy magnitude in the EMSS and Slew samples are illustrated in Fig. 3. The average absolute magnitude of the host galaxies is $\langle M_R(host)\rangle$ = -23.85 ± 0.59 (all), -23.94 ± 0.50 (EMSS) and -23.74 ± 0.68 (Slew), the average scale length of the host is $\langle$R(e)$\rangle$ = 8.9±4.8 kpc (all), 8.8±5.2 kpc (EMSS) and 9.1±4.3 kpc (Slew), while the average absolute magnitude of the nucleus is $\langle M_R(nucleus)\rangle$ = -23.2 ± 1.6 (all), -23.3 ± 1.3 (EMSS) and -23.2 ± 1.9 (Slew). The average host luminosity is in good agreement with previous studies (e.g. $\langle M_R\rangle$ = -23.7 ± 0.7, WSY96; $\langle M_R\rangle$ = -23.7 ± 0.6, U99b) and confirms that the host galaxies of BL Lacs are almost without exception giant ellipticals. No significant difference is found in the distribution of these values between the EMSS and Slew samples. At high luminosities the two distributions are very similar while at lower luminosities Slew hosts appear slightly but not significantly fainter than EMSS sources. This can be due differences in the selection procedure. A K-S test between the two distributions yields P_{KS} = 0.1, confirming that the two distributions are practically indistinguishable.

4.2. Comparison with previous observations of BL Lacs

4.2.1. Comparison with the CFHT survey

Since we have 22 objects in common with the CFHT survey of BL Lac objects (WSY96). it is interesting to compare our results for individual sources with those obtained by WSY96. Of the 22 BL Lacs, three are unresolved by the CFHT and/or the NOT data. Thus, the final comparison is based on 19 resolved sources in common between the NOT and CFHT samples. Before comparing the results we have transformed the WSY96 host magnitudes from the Gunn r–band they used into our Cousins R–band assuming r–R = 0.3 and applying a small correction ($\sim$ 0.1 mag) for the different cosmology used ($q_\circ$ = 0.5 instead of $q_\circ$ =0).

Fig. 4 shows the apparent host magnitudes from the two studies plotted against each other, with a one–to–one correspondence superimposed. On average, the agreement is quite good, even if in few cases the difference is quite large (1.7 mag for 0922+749 and 1.1 mag for 0419). For both these cases there are observations obtained with HST (see the Appendix) that agree with our values within few tens of mag. The average and median difference in the host apparent magnitude is $\langle m_{NOT} - m_{CFHT}\rangle$ = -0.12 ± 0.65 and 0.07, respectively.

4.2.2. Comparison with the HST snapshot survey

We have 40 objects in common with the HST snapshot survey of BL Lac objects (Scarpa et al. 1999b; U99b). Although the NOT and HST data are taken with different instruments and have different spatial resolution, the data have been analyzed homogeneously, facilitating comparison between the samples. Of the 40 BL Lacs, four are unresolved by HST. Of these four sources, 1ES 0647+250, MS 1402.3+0416 and 1ES 1517+656 remain also unresolved by us, while for 1ES 0033+595 we are able to detect a probable nebulosity. This observation is however complicated because of the presence of a very bright star close to the target (see individual notes).

The comparison is therefore based on 35 sources in common between the NOT and HST samples.

Fig. 4 shows the apparent host magnitudes from the two studies plotted against each other, with a one–to–one correspondence superimposed. The average and median difference in the host magnitude with respect to the results of this study are $\langle m_{NOT} - m_{HST}\rangle$ = 0.2 ± 0.4 and 0.1, respectively.

In addition we show in Fig. 5 the comparison of the distributions of the absolute host magnitudes from the two whole surveys. On average the agreement is also very good. The average host and nuclear luminosities of the HST survey are $\langle M_R(host)\rangle_{HST}$ = -23.76 ± 0.57 and $\langle M_R(nucleus)\rangle_{HST}$ = -23.2 ± 1.5. The difference of average and median host luminosity with respect to the results of this study are $\langle M_{NOT}\rangle$-$\langle M_{HST}\rangle$ = -0.1 and -0.2, respectively.

In Fig. 6 we compare the radial profiles observed in this study of three BL Lacs with those derived from HST images (Scarpa et al. 1999b). The three objects were chosen to represent different well resolved (MS 0257.9+3429), poorly resolved (1ES 1218+304) and unresolved sources (MS 1402.3+0416) both in the NOT and HST images. While the HST data allow one to investigate the host much closer to the nucleus, the NOT images are clearly much deeper. This is partly due to the longer exposure times and to the favorable pixel scale of the NOT data. This translates into a better capability for the NOT images of mapping the faint outer regions of the galaxies. Also, Fig. 6 clearly shows the effect of different seeing on the PSF in the

Table 3. Best-fit parameters of the profile fits and properties of the host galaxies.

Name	z	μ_0	r_e ($''$)	m_{nuc} (mag)	m_{gal} (mag)	χ^2	K–cr.	M_{PSF} (mag)	M(host) (mag)	R(e) (kpc)	μ(E)	Note
1ES 0033+595	...	12.00	0.40	18.88	18.92	1.50	...	...	...	...	...	
1ES 0120+340	0.272	14.97	3.40	16.39	17.24	7.17	0.29	-25.19	-24.63	18.89	21.72	a)
MS 0122.1+0903	0.339	13.60	0.90	15.43	18.75	0.52	0.38	-26.65	-23.70	5.79	20.08	
MS 0158.5+0019	0.229:	14.70	2.05	18.82	18.07	0.26	0.32	-22.87	-23.94	12.15	21.45	
MS 0205.7+3509	0.318:	14.50	1.20	17.53	19.03	0.06	0.35	-24.48	-23.33	7.41	20.99	a)
1ES 0229+200	0.139	13.84	4.00	18.25	15.76	0.04	0.13	-21.91	-24.53	13.33	21.06	
MS 0257.9+3429	0.247	14.44	2.05	19.07	17.81	1.32	0.27	-22.45	-23.98	10.64	21.13	
MS 0317.0+1834	0.190	12.70	1.10	19.01	17.42	4.10	0.20	-21.93	-23.72	4.70	19.61	a)
1ES 0347-121	0.188	11.80	0.65	19.37	17.66	1.16	0.20	-21.26	-23.17	2.76	19.01	
1ES 0414+009	0.287	12.54	1.00	16.97	17.47	0.41	0.31	-24.91	-24.72	5.76	19.05	
MS 0419.3+1943	0.512:	14.10	0.74	18.65	19.68	3.31	0.75	-25.12	-24.84	6.05	19.04	
1ES 0446+449	0.203:	16.11	22.90	...	14.24	...	0.21	...	-29.13	102.92	20.90	
1ES 0502+675	0.341	10.98	0.35	16.83	18.19	5.25	0.38	-25.60	-24.62	2.26	17.12	a)
1ES 0525+713	0.249:	14.35	2.30	...	17.47	1.27	0.27	...	-24.34	12.01	21.03	
MS 0607.9+7108	0.267	14.1	1.85	18.31	17.69	1.35	0.29	-23.40	-24.31	10.1	20.7	
1ES 0647+250	...	...	...	15.03	...	12.95	0.21	...	...	...	...	
MS 0737.9+7441	0.315	12.97	1.10	18.29	17.69	4.01	0.34	-23.58	-24.52	6.75	19.60	
1ES 0806+524	0.136:	12.05	1.70	15.77	15.83	2.32	0.13	-24.16	-24.24	5.63	19.48	
MS 0922.9+7459	0.638:	15.26	1.03	20.34	20.12	16.87	1.15	-23.30	-24.67	9.40	20.17	
1ES 0927+500	0.188	15.50	3.00	17.65	18.04	2.20	0.20	-22.89	-22.70	12.72	22.80	
MS 0950.9+4929	$>$0.5	...	...	18.78	...	0.04	0.22	$<$-21.95	...	...	...	
MS 0958.9+2102	0.334	15.18	1.82	20.66	18.81	0.10	0.37	-21.30	-23.52	11.60	21.76	
1ES 1011+496	0.210	14.37	2.73	16.07	17.12	15.92	0.21	-24.58	-23.74	12.13	21.64	
1ES 1028+511	0.239:	13.75	1.30	16.69	18.11	5.27	0.26	-24.39	-23.23	6.59	20.83	
1ES 1106+244	...	15.60	1.40	18.71	19.8	5.35	0.48	...	...	...	21.93	a)
1ES 1118+424	0.124:	...		16.88	...	1.83	0.11	-22.71	...	...	...	
1ES 1212+078	0.130	14.64	5.51	17.26	15.86	0.33	0.12	-22.42	-23.94	17.38	22.23	
1ES 1218+304	0.182:	13.55	2.17	16.32	16.8	0.18	0.19	-24.14	-23.85	8.97	20.88	
MS 1221.8+2452	0.218:	12.46	0.62	17.76	18.43	75.64	0.23	-23.15	-22.71	2.94	19.60	
MS 1229.2+6430	0.164	13.51	2.90	17.35	16.13	2.06	0.17	-22.89	-24.28	11.05	20.91	
MS 1235.4+6315	0.297	13.80	1.39	19.20	18.01	0.11	0.32	-22.43	-23.95	8.20	20.60	
1ES 1255+244	0.141	13.10	1.90	18.27	16.64	1.23	0.14	-21.59	-23.36	6.41	20.63	
MS 1256.3+0151	...	...	...	19.50	...	0.14	...	...	...	...	...	
MS 1402.3+0416	0.344:	...	...	16.88	...	0.60	0.39	-25.14	...	...	...	
MS 1407.9+5954	0.495	14.80	1.00	18.69	19.73	5.53	0.70	-24.23	-23.89	8.04	20.60	
MS 1443.5+6349	0.299	15.49	2.90	19.38	18.11	2.90	0.32	-22.27	-23.86	17.18	22.28	
MS 1458.8+2249	0.235:	10.50	0.46	16.27	17.12	0.98	0.25	-24.89	-24.29	2.30	17.49	
1ES 1517+656	$>$0.7	...	...	16.38	...	6.86	1.35	$<$-27.49	...	...	...	
MS 1534.2+0148	0.312	15.81	4.05	19.22	17.7	10.38	0.34	-22.70	-24.56	24.68	22.38	b)
MS 1552.1+2020	0.222	13.80	2.35	17.97	16.87	0.59	0.24	-23.05	-24.39	11.29	20.84	
MS 1704.9+6046	0.280	14.95	2.40	19.49	17.98	0.20	0.30	-22.02	-23.83	13.60	21.80	
MS 1757.7+7034	0.407	12.14	0.30	17.89	19.68	0.84	0.50	-24.65	-23.36	2.16	18.28	a)
1ES 1853+671	0.212	15.64	2.50	19.47	18.58	0.51	0.23	-21.53	-22.65	11.61	22.64	
1ES 1959+650	0.048:	13.25	4.10	14.86	15.12	10.85	0.04	-22.97	-22.75	5.34	20.85	
1ES 2037+521	0.05?	14.86	5.80	19.64	15.97	2.17	0.04	-20.01	-23.72	7.84	20.72	
MS 2143.4+0704	0.237	14.62	2.17	18.24	17.87	0.18	0.26	-22.99	-23.62	10.94	21.54	
1ES 2321+419	0.059:	...	...	17.31	...	1.35	0.05	-20.94	...	...	...	
1ES 2326+174	0.213	13.06	1.60	18.41	16.97	2.42	0.23	-22.51	-24.18	7.46	20.15	
MS 2336.5+0517	...	12.60	0.60	19.83	18.64	0.08	...	...	...	...	...	
1ES 2343-151	0.226	13.27	1.60	20.36	17.18	0.67	0.24	-20.63	-24.05	7.79	20.37	b)
1ES 2344+514	0.044	12.87	5.80	17.00	13.98	0.25	0.03	-20.89	-23.95	6.96	20.24	
MS 2347.4+1924	0.515	13.27	0.40	21.89	20.19	0.75	0.76	-21.26	-23.72	3.28	18.83	

a) elliptical fit preferred but disk fit not ruled out
b) poor fit in the external outer region

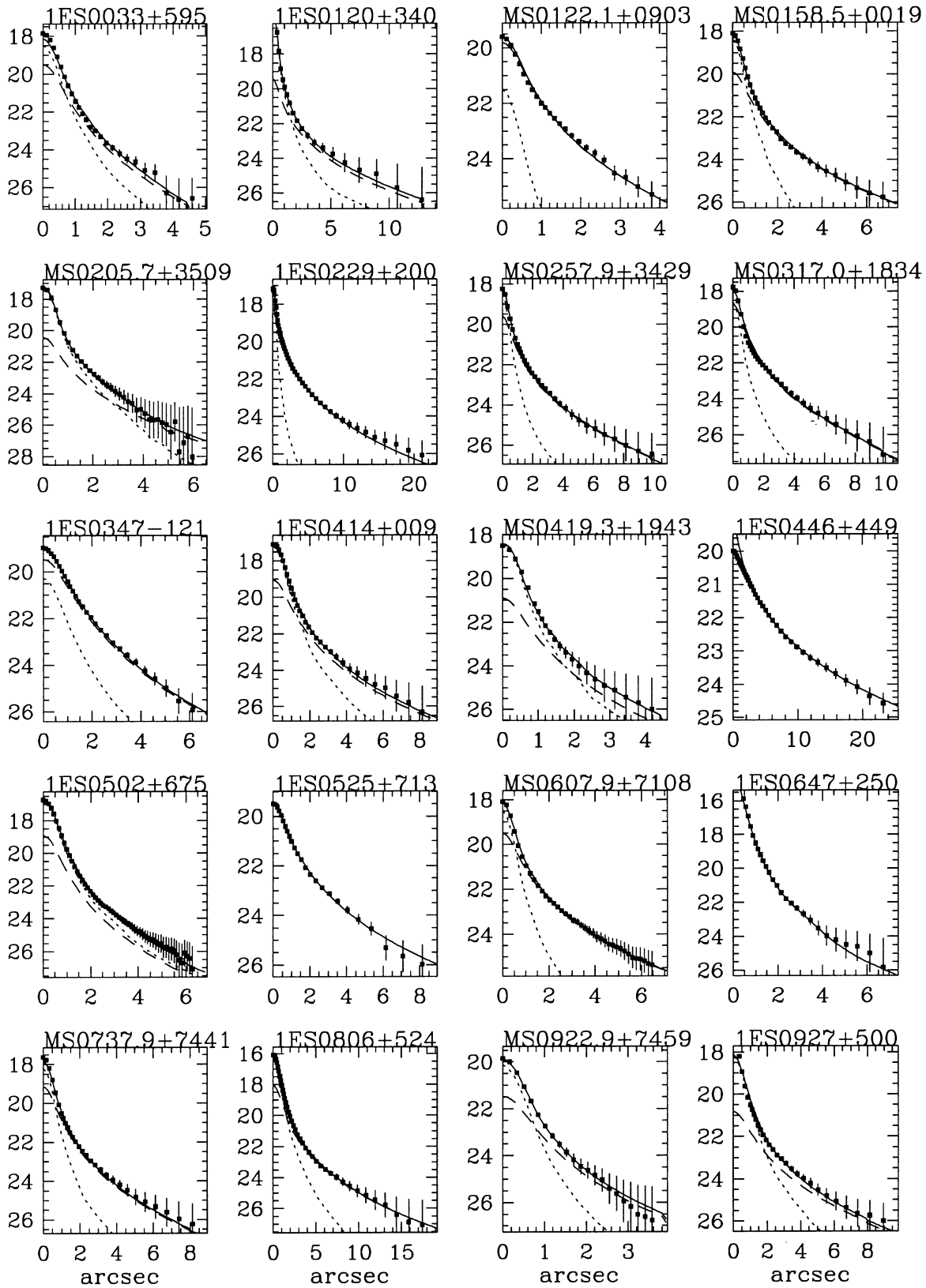

Fig. 2. The observed radial luminosity profiles of each BL Lac object (filled squares), superimposed to the fitted model consisting of the PSF (short-dashed line), de Vaucouleurs bulge (medium-dashed line) and/or exponential disk (long-dashed line). The solid line shows the total model fit.

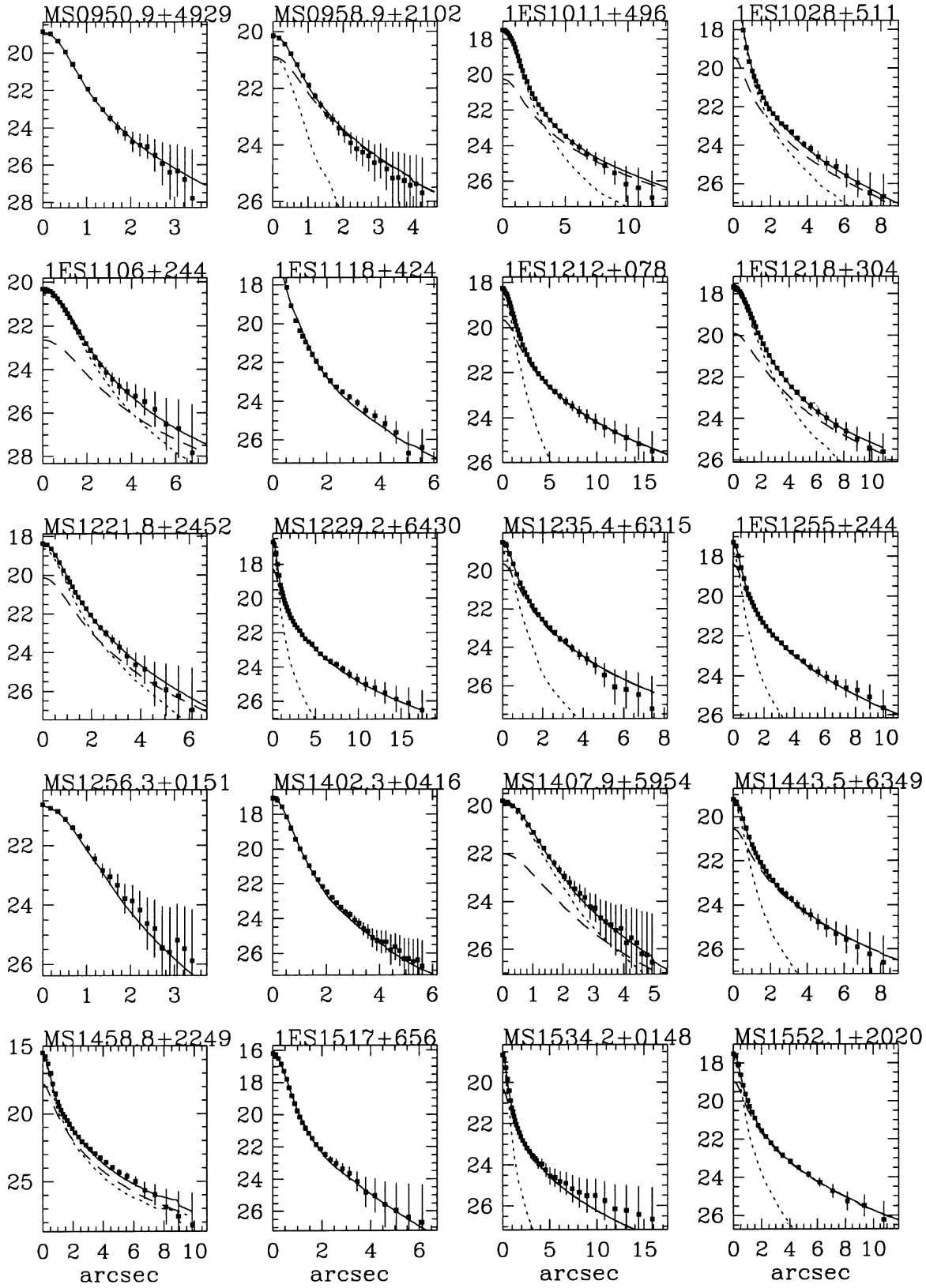

Fig. 2. (continued)

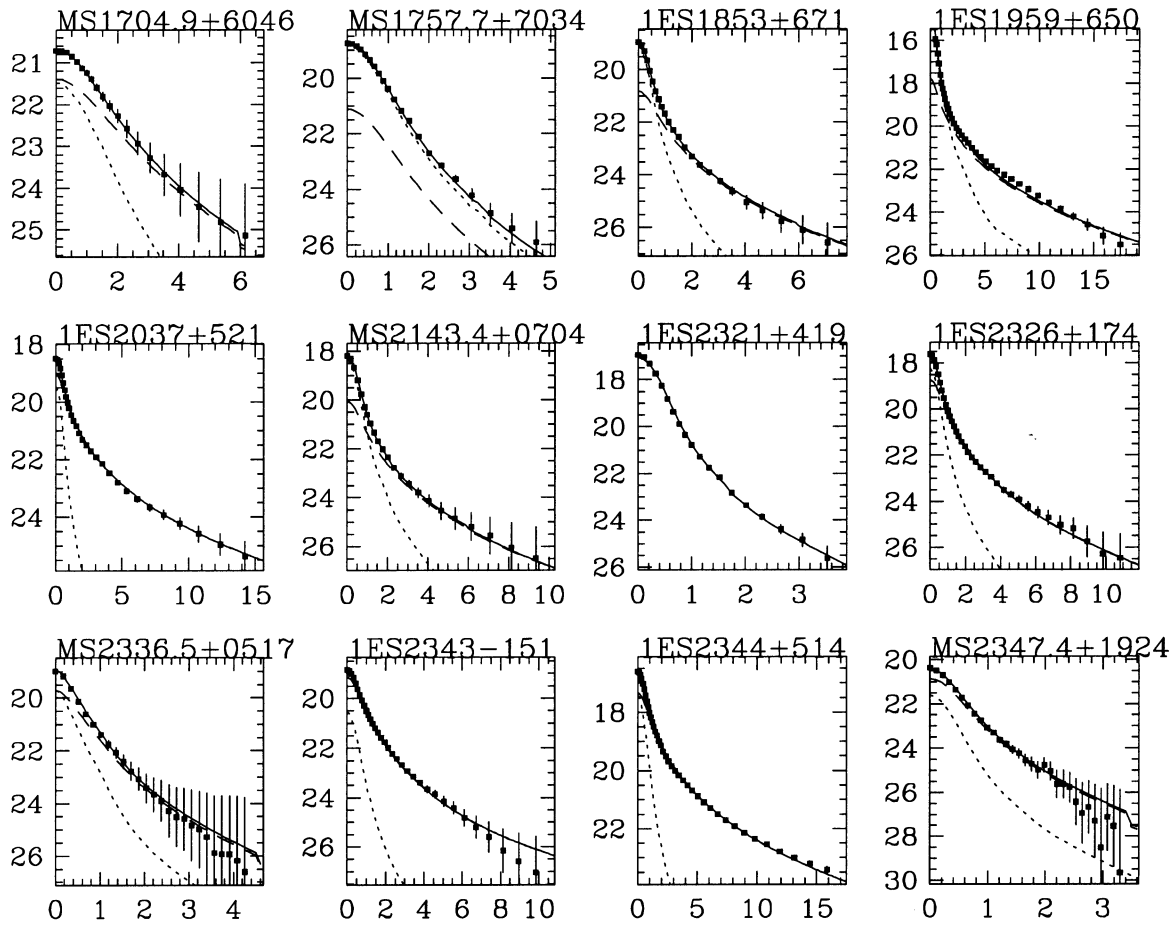

Fig. 2. (continued)

ground based images (0.″5 for MS 0257.9+3429 and 1.″0 for 1ES 1218+304). An optimal characterization of the host galaxies would thus be obtained by combining the high resolution (HST) images with the deeper ground-based observations. The relevance of this point in a larger sample of BL Lacs will be discussed in a forthcoming paper.

4.3. Comparison with radio galaxies

According to the unified schemes of radio-loud AGN (see e.g. Urry & Padovani 1995), BL Lacs and RGs of F-R I type morphology are identical objects seen along different angles with respect to the relativistic jet. A number of optical studies have reported on the optical properties of RGs (see Govoni et al. 1999 and references therein). These have almost unanimously found that hosts are luminous ellipticals sometimes interacting with other galaxies, other times rather isolated. A general trend has been reported suggesting that F-R I RGs are on average brighter and in denser environments than those hosting F-R II RGs. Comparison among various samples is hindered by the selection procedure and by possible systematic effects introduced by the analysis (e.g. extinction, K-correction, passband, method of measurement of galaxy magnitude, etc). In order to reduce as much as possible the systematic effects we compare our results with those obtained by Govoni et al. (1999) for a large sample of low redshift RGs. This sample includes 79 RGs of both F-R I and F-R II type in the redshift interval 0.01 to 0.1. R–band imaging is used to investigate in detail the morphological and photometric properties of the radio galaxies. This includes the analysis of the luminosity profile using the same procedure and the corrections used in this work.

The average host luminosity of the F-R I and F-R II RG hosts are $\langle M_{FRI} \rangle$ = -24.1±0.6 and $\langle M_{FRII} \rangle$ = -23.6±0.7. The BL Lac hosts appear therefore on average slightly brighter than F-R II hosts, but also slightly fainter than the F-R I RG hosts, which are in turn quite similar to BCGs in moderately rich clusters at z<0.15 ($\langle M_{BCG} \rangle = -24.1 \pm 0.3$; Hoessel et al. 1980). Note that since the RGs are at lower redshift, any cosmological evolutionary correction makes the difference from FR I even larger. A similar trend was also noted by Lamer et al. (1999) comparing BL Lacs and FR I galaxies in the near infrared.

On the other hand the comparison between BL Lac hosts and the whole sample of RG shows a general good agreement. In Fig. 7 we report the histogram and cumulative distribution of the absolute host magnitudes of the BL Lacs and the RGs from Govoni et al. (1999). The two distributions are rather similar with only a significant excess of more bright RG that are not present in the BL Lacs. If we compare BL Lacs with F-R I and

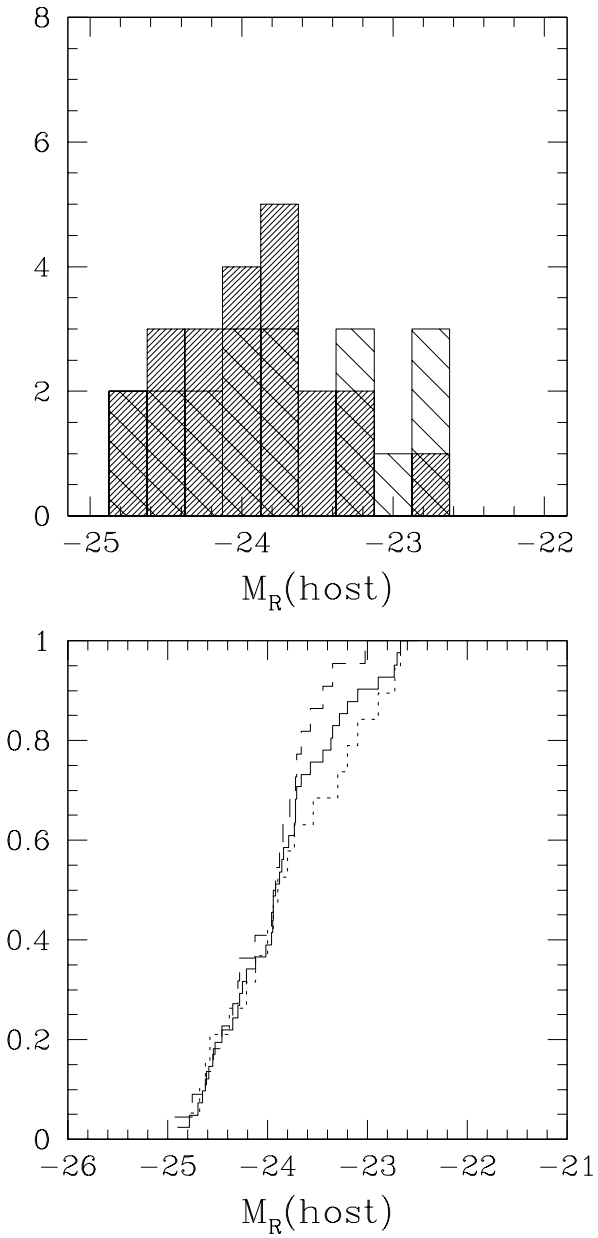

Fig. 3. *Top:* Histogram of the absolute host galaxy magnitudes of the BL Lacs (thickly-hatched EMSS sample;thinly-hatched Slew sample). *Bottom:* Cumulative distributions for: All objects (solid line), EMSS (long-dashed line) and Slew (short-dashed line).

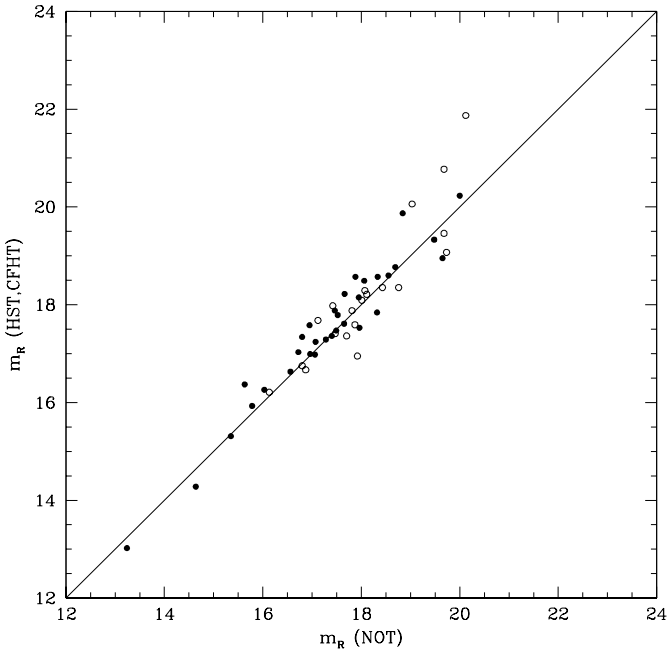

Fig. 4. Comparison of the apparent host galaxy magnitudes derived in this study for those BL Lacs in common with the CFHT survey (WSY96; open circles) and with the HST snapshot survey (U99b; full circles). A one–to-one correspondence is shown as a solid line.

F-R II separately the agreement is formally good for F-R II but not for F-R I. A K-S test yields formally P_{KS} = 0.250 and 0.004 for F-R II and F-R I respectively compared with BL Lac host luminosities.

Since the selection procedure that identifies samples of BL Lacs and of RG is different, we cannot rule out that selection effects may introduce some bias. These effects should be related to correlations between host optical luminosity and X-ray and radio properties which are used to classify the objects.

The present result indicates that from the point of view of host luminosities either the parents of BL Lacs are RG of both types (I and II) or for some reason brightest F-R I must be excluded from the parent population as proposed by WSY96.

The first association of BL Lacs with F-R I was done on the basis of similar extended radio emission (Browne 1983, Wardle et al. 1984; Antonucci & Ulvestad 1985). There are however some observations (e.g. Kollgaard et al. 1992, Murphy et al. 1993) that indicate that at least some BL Lac object may have diffuse emission more similar to that of F-R II than F-R I. The same conclusion is reached from the kpc scale radio polarization study of six BL Lacs (Stanghellini et al. 1997) where the magnetic field is parallel to the radio jet axis for most of its length as found in F-R II sources. If the radio morphology of these BL Lacs be of F-R I type the magnetic field should be dominated by the component perpendicular to jet axis.

Our results therefore are consistent with the idea that BL Lacs avoid the BCGs in rich clusters at low redshift (Wurtz et al. 1997) although there are examples of BL Lacs in very luminous hosts and members of group/clusters of galaxies (see 1ES 0414+009 and PKS 0548-322; this study and Falomo et al. 1995; 1Es1741+196 Heidt et al. 1999). This idea is also supported by the narrow-angle tail radio morphology seen in many BL Lacs and non-BCGs (e.g. Owen & Laing 1989; Perlman & Stocke 1993) and by the correlation between cluster richness and the BCG and BL Lac luminosity (Thuan & Romanishin 1981; Wurtz et al. 1997).

On the other hand evidence is growing that also from the point of view of the extended radio luminosities many BL Lacs are quite different from FR I and share the characteristic luminosity of FR II sources (Cassaro et al. 1999). This evidence

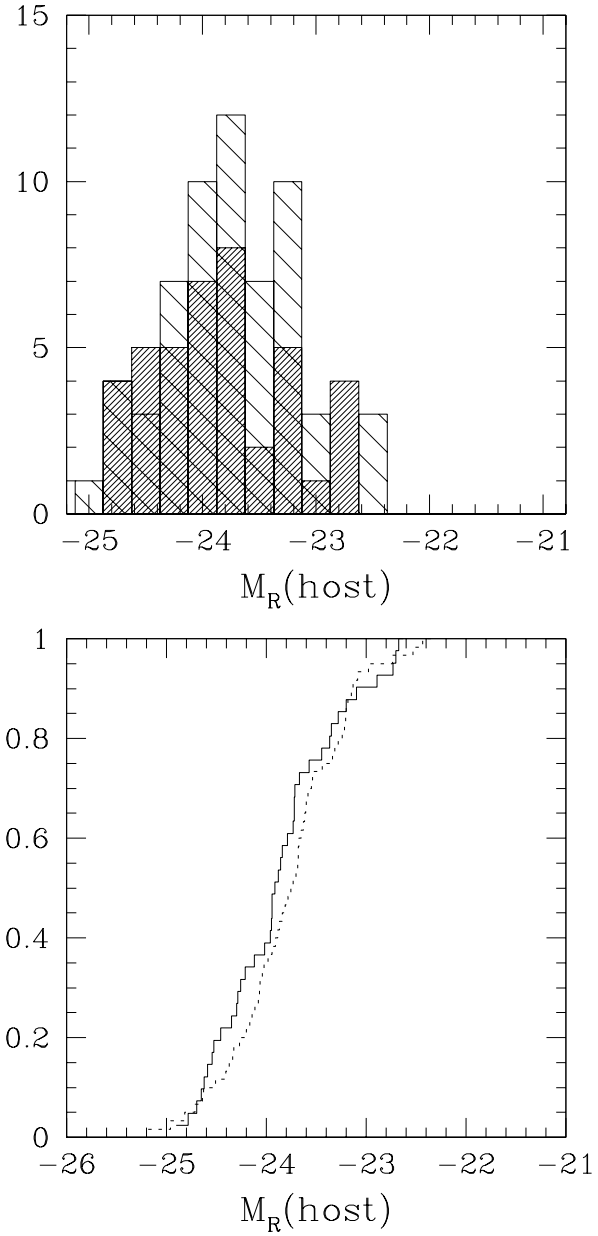

Fig. 5. Histogram and cumulative distribution of the absolute host galaxy magnitudes of the BL Lacs in this study (thickly hatched; solid line) and the whole HST snapshot survey (U99b; thinly hatched; short-dashed line.

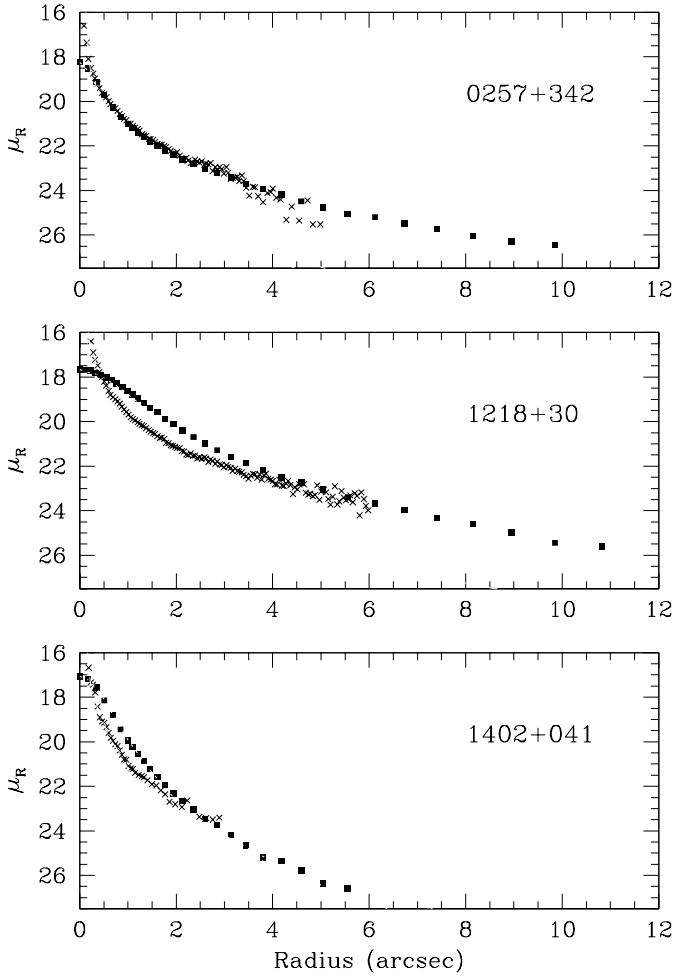

Fig. 6. Comparison of the radial luminosity profiles of selected BL Lacs derived from the NOT images (filled squares) and from the HST images (crosses). For comparison, a PSF profile matching the nucleus is plotted for both the NOT (dotted line) and the HST images (dashed line). Different representative cases are shown: a well resolved object (top panel), a poorly resolved object (middle panel) and an unresolved object (bottom panel).

together with our results on the host luminosities led to argue that both types of RG form the parent population of BL Lacs.

4.4. The Fundamental Plane and Hubble diagram

It is well established that elliptical galaxies form families of homologous systems with characteristic parameters R(e), μ(e) and velocity dispersion σ. These are commonly represented in the Fundamental Plane (see e.g. Djorgovski & Davis 1987). We have investigated the properties of the BL Lac hosts in the projected Fundamental Plane (F-P) concerning the central surface brightness μ(e) and the scale length R(e). Surface brightness μ(e) derived from the fit (see Table 3) was corrected for Galactic extinction, K–correction and for the $(1+z)^4$ cosmological dimming. Fig. 8 shows the correlation between μ(e) and log R(e) for the BL Lac hosts and the low redshift RG hosts (Govoni et al. 1999). It can be seen that the behavior of the EMSS and Slew BL Lac hosts are similar. Both BL Lac hosts and the RG hosts (Govoni et al. 1999) follow the Kormendy relation for giant massive ellipticals (e.g. Capaccioli et al. 1992), with a best-fit correlation μ(e) = 16.45 + 4.6 $\times$ (log R(e)). Practically no host galaxy is in the (scatter) area at log R(e) $<$ 0.5 kpc. This confirms that the BL Lac hosts are almost exclusively drawn from the population of giant ellipticals and not from normal field ellipticals. Note that the BL Lac hosts seem to avoid the area of the brightest and largest galaxies in the bottom right hand corner of Fig. 8, similarly to the result based on the total host luminosities (Fig. 7).

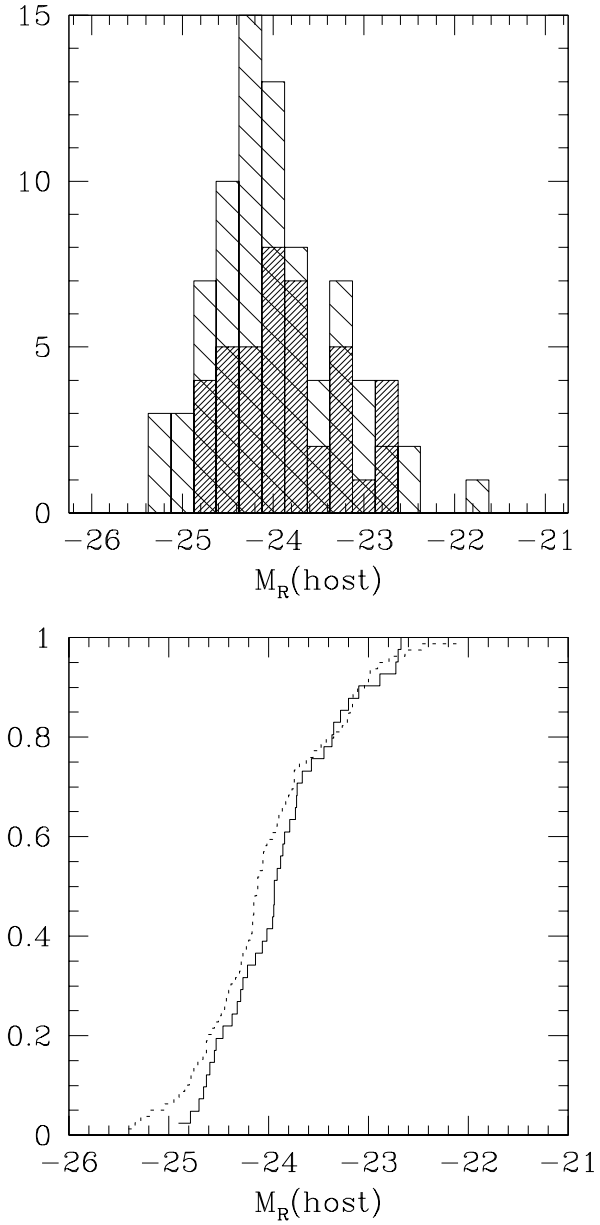

Fig. 7. Histogram and cumulative distribution of the absolute host galaxy magnitudes of the BL Lacs in this study (thickly hatched; solid line) and the RGs (Govoni et al. 1999; thinly hatched; short-dashed line).

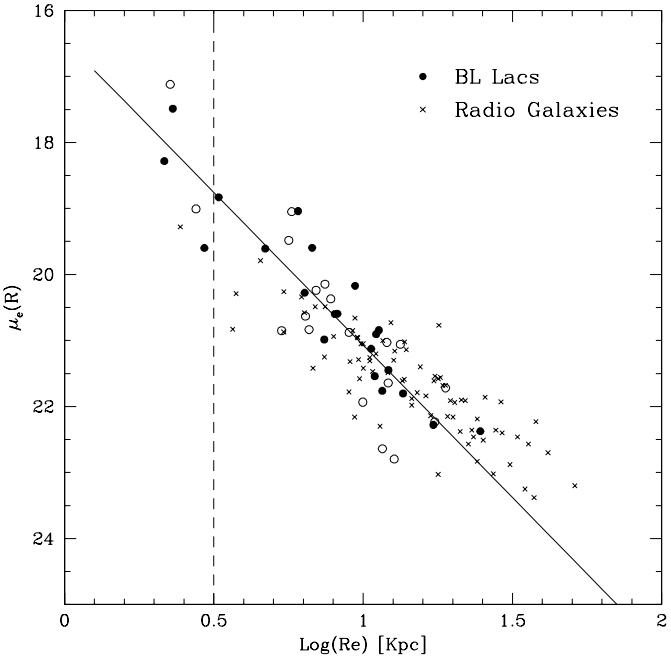

Fig. 8. Kormendy relation for BL Lac host galaxies: EMSS (full circles)and Slew (open circles) objects are compared with RG hosts (Govoni et al. 1999; crosses). The solid line shows the best fit, while the dashed line shows the dividing line between normal and giant ellipticals (Capaccioli et al. 1992).

In Fig. 9 we show the apparent R magnitude vs. redshift Hubble diagram for the BL Lac hosts (this work), together with data for RGs (Govoni et al. 1999), compared with the expected relationship for elliptical galaxies derived from passive stellar evolution models (Bressan et al. 1994) normalized to the average redshift and magnitude of the low redshift RGs from Govoni et al. 1999). The resolved BL Lac hosts lie within about 1 mag spread on the H–z relation, as do the RGs. Based on this diagram we can estimate the redshift of the four objects with unknown redshift but resolved in our images. These are 0033+59, 1106+24, 2037+52, and 2336+05 (see Fig. 9) for which we derive a Hubble law redshift of 0.43, 0.58, 0.14 and 0.40 respectively.

4.5. Luminosities of the host and the nucleus

Optical images of BL Lacs are characterized by the superposition of two components: the extended starlight emission from the galaxy and the non-thermal unresolved bright nucleus. We discuss here the properties of these two components as derived from our sample.

Fig. 10 shows the relationship between absolute magnitude of hosts and redshift of our BL Lacs and of other samples of AGN. All BL Lac hosts at all redshifts have luminosities between that of a passively evolving M* and M*–2 mag galaxies, where M* is the characteristic luminosity of a Shechter luminosity function. While there are RG hosts (Govoni et al. 1999) with luminosities larger than M*–2, none of the observed BL Lacs are found in such a luminous galaxy. Note that any correction due to different average redshift would make this difference even larger. There is a suggestion of a positive correlation of host luminosity with redshift, consistently with what is expected from passive stellar evolution models for elliptical galaxies (e.g. Bressan et al. 1994; Fukugita et al. 1995), and the evolution of galaxies in clusters (Ellingson et al. 1991), although the scatter is large. This trend is similar to that suggested by WSY96 and is consistent with the average value found for higher redshift flat spectrum radio quasar (FSRQ) host galaxies (Kotilainen et al. 1998a): $\langle z \rangle_{FSRQ}$ = 0.673, $\langle M_{host} \rangle_{FSRQ}$ = −25.3 and even

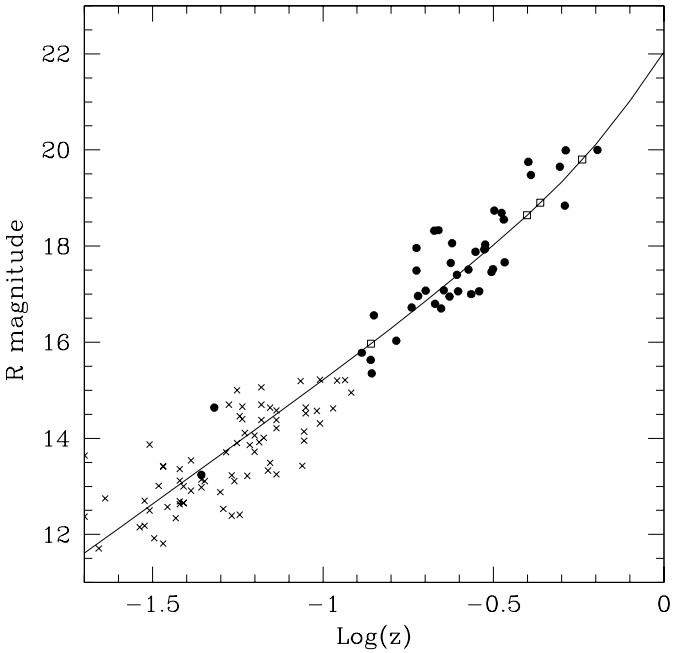

Fig. 9. Hubble diagram for BL Lac hosts (filled circles) and RGs (crosses) by Govoni et al. 1999. The solid line shows the expected behavior for a massive elliptical galaxy undergoing passive stellar evolution (Bressan et al. 1994). The expected position on the Hubble diagram for the four resolved BL Lacs with unknown redshift are marked with open squares (see text).

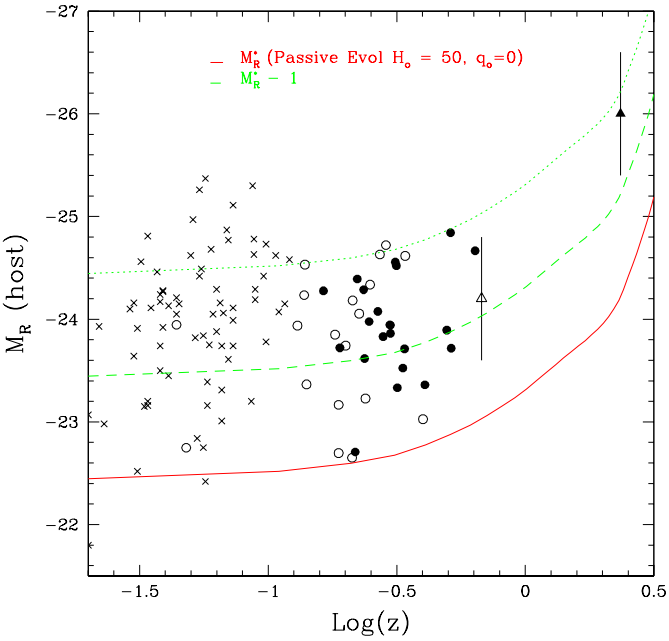

Fig. 10. Correlation between the absolute host magnitude of the BL Lacs in EMSS (full circles) and Slew (open circles) with redshift. Solid, dashed and dotted lines show a passively evolving M^*, M^*–1 and M^*–2 mag galaxy, respectively (Bressan et al. 1994). Also plotted are RGs from Govoni et al. 1999 (crosses) and the average values for FSRQs (open triangles; Kotilainen et al. 1998a) and high z RLQs (filled triangles; Lehnert et al. 1992).

with high redshift RLQs (Lehnert et al. 1992): $\langle z \rangle_{RLQ}$ = 2.34, $\langle M_{host} \rangle_{RLQ}$ = −26.3.

Fig. 11 shows the histogram of the ratio between nuclear and host luminosity for the resolved BL Lac objects. This ratio ranges from 0.03 to 3, with average ∼0.8 and median ∼0.4. Interestingly, we find an apparently bimodal distribution with two peaks around log(LN/LH) ∼–0.6 and log(LN/LH) ∼0.2. This behavior is present in both the EMSS and Slew sub-samples.

While the detected large range in the luminosity ratio within individual objects can be due to differences in the intrinsic nuclear or host luminosity, or a difference in the beaming factor from one object to another, it is difficult to explain the apparent bimodality present in both EMSS and Slew samples.

In comparison, the luminosity ratio in the V–band for the low redshift quasars studied by Bahcall et al. (1997) is ∼10 while for the RGs observed in the R–band (Govoni et al. 1999) this ratio is less than 0.1. For BL Lacs therefore the observed nuclear optical luminosity seems intermediate between that of RG and quasars.

In order to investigate the relationship of the optical nuclear luminosity with that in different bands we have performed a partial correlation analysis among radio, optical, and X-ray luminosities. We used data in Table 1 together with nuclear optical data of Table 3 and used the procedure described in Padovani (1992). For all objects with known redshift we computed the Spearman rank order correlation coefficients between luminosities and between luminosity in a given band and redshift. The results of the correlation analysis are given in Table 4. It turns out

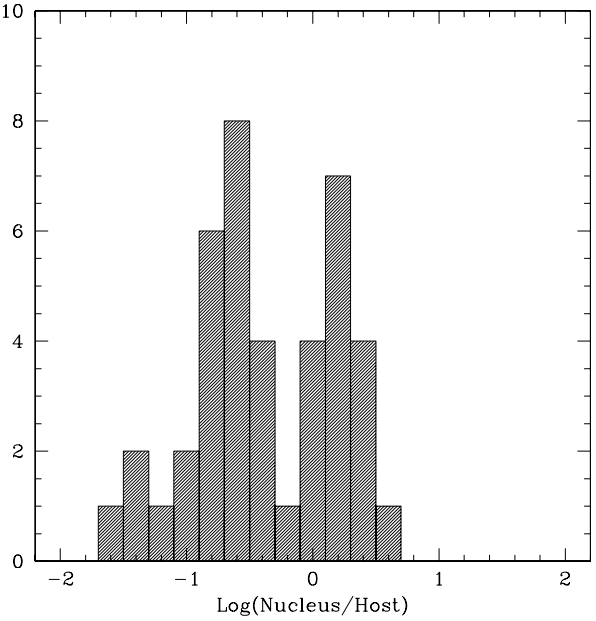

Fig. 11. Histograms of the ratio between nuclear and host luminosity for resolved BL Lac objects.

that apart the weak correlation with redshift (which is marginally significant only for L_x) the only significant correlation among luminosities after subtraction of the redshift dependency is between L_o and L_r. A similar result was obtained from the analysis

Table 4. Correlation coefficients for BL Lacs luminosities.

	L_r	L_o	L_x	z
L_r	1.0	0.74	0.55	0.30
L_o	...	1.0	0.48	0.27
L_x	...	...	1.0	0.45
z	...	...	...	1.0

of a smaller sample of X-ray BL Lacs by Padovani (1992) but with a smaller correlation coefficient.

Fig. 12 shows the relationship between the absolute host and nuclear magnitudes of the BL Lacs in EMSS and Slew. There is an indication of a weak correlation (Spear correlation coefficient. = 0.3) between the two parameters, in the sense that more luminous nuclei reside in more luminous hosts.

However, we note the obvious selection effects that may depopulate the upper left hand (faint nuclei in luminous hosts) and lower right hand (faint hosts swamped by luminous nuclei) corners of the diagram. While the first effect could bias the original samples (see e.g. Browne & Marcha 1993) the second should have marginal effect since, excluding misclassified objects we are able to resolve 90% of observed targets.

The putative correlation is, however, consistent with the luminosity/host-mass limit found when considering AGN samples at higher redshift and with more luminous nuclei and hosts (Kotilainen et al. 1998a; Lehnert et al. 1992). Also, assuming that BL Lac activity results from accretion of material onto a super-massive black hole, it is in agreement with the relationship found by Magorrian et al. (1998) from HST kinematic study between the mass (luminosity) of the black hole and the mass (luminosity) of the spheroid component in nearby galaxies. McLure et al. (1999) detected a similar weak correlation for a small sample of 9 RLQs at z$<$0.35, and calculated that most of their RLQs radiate at a few percent of the Eddington luminosity. The correlations found in this study and in McLure et al. (1999) indicate that the Magorrian et al. relationship extends to galaxy and host galaxy masses at cosmological distances. On the other hand the lack of a strong correlation found in this study of relatively nearby and modest luminosity AGN may indicate that the onset of the correlation occurs only after a certain level in nuclear and/or galaxy luminosity has been reached (cf. with Kotilainen et al. 1998a).

5. Conclusions

We have presented high resolution homogeneous optical observations of a large data set of BL Lac objects drawn from two complete samples of X–ray selected (high frequency peaked) sources. We are able to resolve $\sim$ 90% of the observed targets and study the properties of their host galaxies. It turns out that all galaxies are well represented by elliptical model with mean luminosity $\langle M_R(host)\rangle$ = $-$23.9 and an observed average nuclear source-to-host luminosity ratio of $\sim$ 1. It is also shown that hosts of BL Lacs are almost exclusively drawn from the population of massive elliptical galaxies. No cases of disc dominated systems hosting BL Lacs are found supporting the view that all radio-loud active galaxies are dominated by the spheroidal component.

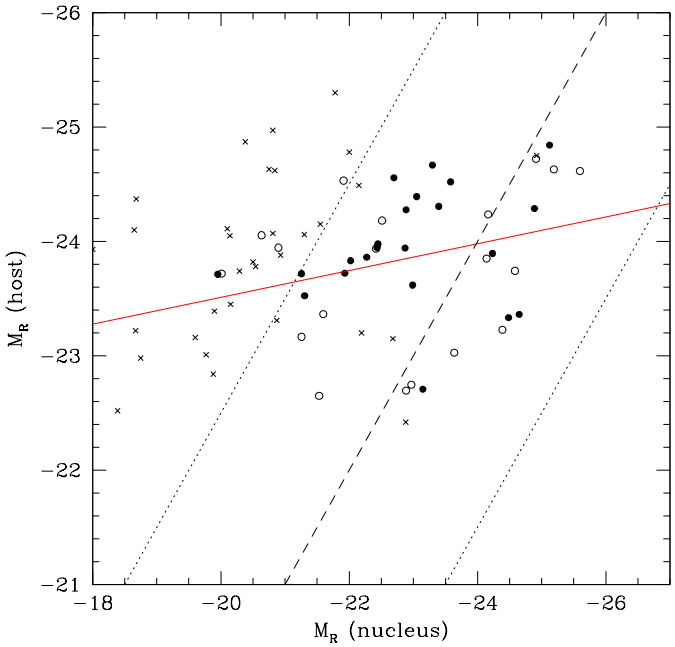

Fig. 12. Absolute host galaxy magnitude plotted against absolute nuclear magnitude of the resolved BL Lacs: EMSS (full circles) and Slew (open circles). Also plotted are values for low redshift RGs (crosses) by Govoni et al. Solid line is a simple regression fit to the all data. Dashed line is the one to one relationship while dotted lines represent loci in the diagram with luminosity ratio = 0.1 and 10.

The global properties of the galaxies hosting BL Lacs follow the same relationships of normal (non active) giant ellipticals under passive stellar evolution. The comparison of properties of BL Lac hosts with those of low redshift radio galaxies indicates that from the point of view of galaxy luminosity both FR I and FR II radio galaxies form the parent population of BL Lacs. A result that is supported recent radio imaging and polarization studies that show many BL Lacs exhibiting the characteristics of FR II sources.

Acknowledgements. This work was partly supported by the Italian Ministry for University and Research (MURST) under grant Cofin98-02-32. This research has made use of the NASA/IPAC Extragalactic Database (NED) which is operated by the Jet Propulsion Laboratory, California Institute of Technology, under contract with the National Aeronautics and Space Administration.

Appendix A: notes on individual objects

A.1. Unresolved BL Lacs

In spite of the good seeing conditions seven BL Lacs remained unresolved. For all these objects the redshift is unknown or uncertain. For two unresolved BL Lacs (MS 0950.9+4929 and 1ES 1517+656), the redshift (or lower limit of redshift) is high enough to explain the lack of detection of the host galaxy. For the other five unresolved objects (1ES 0647+250, 1ES 1118+424, MS 1256.3+0151 MS 1402.3+0416 and 1ES 2321+419), there

are only tentative redshifts which are, however, inconsistent with the results from our images.

We determined a lower limit of the redshift assuming these objects are surrounded by a typical elliptical host galaxy as found in this study (M(R) = -23.8 and R(e) = 10 kpc). A simulated galaxy was produced and superposed onto the image of the observed sources assuming various redshifts. This produced images of the object that appeared resolved or not depending on the redshift used. A lower limit of the redshift was set when the galaxy becomes undetectable. Of course using host galaxies that are less luminous and smaller would make these limits lower.

The derived lower limits for the unresolved BL Lacs are: z $>$ 0.3 for 1ES 0647+250, z $>$ 0.6 for MS 0950.9+4929, z $>$ 0.5 for 1ES 1118+424, z $>$ 0.65 for MS 1256.3+0151, z $>$ 0.5 for MS 1402.3+0416, z $>$ 0.45 for 1ES 1517+656 and z $>$ 0.45 for 1ES 2321+419. With the exception of 1ES 0647+250, the observed magnitude of these objects is consistent with them being at moderately high redshift, thus remaining unresolved. The case of 1ES 0647+250 could be due to either a very bright (or beamed) nucleus or an under-luminous host galaxy. Since some of these BL Lacs have tentative redshift (see individual notes) either these objects are hosted by an atypically faint host galaxy or, more likely, the redshift is wrong.

1ES 0647+250: A tentative redshift z = 0.203 has been derived for this BL Lac, which is unresolved in the NOT images taken with very good seeing (FWHM 0.″65). It is also unresolved in the HST snapshot survey (Scarpa et al. 1999b), who derived an upper limit m(host) $>$19.1. At z = 0.203, this corresponds to M(host) $>-$21.7, i.e. 2 magnitudes fainter than an average BL Lac host.

MS 0950.9+4929: This BL Lac, for which a lower limit to the redshift of z $>$ 0.5 has been derived (Perlman, priv. comm.), remains unresolved in the NOT data, even in good seeing. It was also unresolved by WSY96, who derived an upper limit m(host) $>$19.2. The corresponding absolute luminosity limit from WSY96 is M(host) > -24.4, in good agreement with the average value of the BL Lac hosts derived here.

1ES 1118+424: This BL Lac, at an uncertain redshift z = 0.124 (Perlman et al., priv. comm), remains unresolved in the NOT data, even in very good seeing (FWHM 0.″60). The redshift is inconsistent with results from our image.

MS 1256.3+0151: This BL Lac, at tentative redshift z = 0.162, is unresolved in the NOT data but the seeing during this observation was rather poor (FWHM 1.″34). However, even taking into account the poor seeing, if it is at z = 0.162 its host galaxy should be easily detectable (unless it is atypically faint). We estimate it should be at $z > 0.5$ if hosted by a standard galaxy.

MS 1402.3+0416: This BL Lac, at a tentative redshift z = 0.344, remains unresolved in the NOT data. It was also unresolved by WSY96, who derived an upper limit m(host) $>$18.4, which at z = 0.344 corresponds to M(host) > -23.9. Similarly, it remained unresolved in the HST snapshot survey (Scarpa et al. 1999b), who derived an upper limit m(host) $>$19.4, which at z = 0.344 corresponds to M(host) > -22.9. These upper limits still allow for the existence of a typical elliptical host galaxy which at the moderately high redshift remains unresolved.

1ES 1517+656: This BL Lac, for which Beckmann (priv. comm.) has derived a spectroscopic lower limit of z $>$0.7 based on the presence of MgII and FeII absorption lines, remains unresolved in the NOT data, even in good seeing (FWHM 0.″70). It was also unresolved in the HST snapshot survey (Scarpa et al. 1999b), with an upper limit m(host) $>$19.9, which at z $>$0.7 corresponds to M(host) < -25.2. At this upper limit the observations are consistent with the presence of a luminous host galaxy. At HST resolution, this BL Lac shows an unusual morphology with three non homogeneous arclets surrounding the point source at 1–2 arcsec of distance (Scarpa et al. 1999a). We are able to see clearly the more external arc and can detect the two more internal features after subtraction of a scaled PSF. Our deeper images show that at least the most external ring does not extend more than what it is seen on HST data. Moreover we detect many other faint sources in the immediate 5 arcsec environment.

It was proposed that these arcs are effects of gravitational lensing produced by a foreground galaxy. Our image is much deeper than that obtained with HST but no signature of foreground galaxy is found. This therefore weakens the lens hypothesis.

1ES 2321+419: This BL Lac, at a tentative redshift z = 0.059, remains unresolved by our images. Since the seeing conditions were very good (FWHM 0.″69) we believe the correct redshift is considerably larger than that proposed.

A.2. Misclassified BL Lacs?

1ES 0446+449: This BL Lac at a tentative redshift z = 0.203 was resolved by the HST snapshot survey (Scarpa et al. 1999b), but no point source was detected while a pure exponential (disk) brightness profile was observed. The NOT data confirm that no point source is present in this object. Instead, we detect a very luminous galaxy with m(host) = 15.1, corresponding to an extremely luminous galaxy ($M_R = -29.1$ at the proposed redshift) making it a very unusual source. However, a more likely explanation is that the correct redshift for this object is much lower than z = 0.203 and that this source is not a BL Lac object. From re-inspection of the optical spectrum for this object (Perlman et al. 1996), we note that the redshift determination is probably wrong and the correct redshift is z$\sim$0.02, which would make the identified counterpart to be a normal low redshift elliptical galaxy, and not a BL Lac object.

1ES 0525+713: The NOT data failed to detect a point source at the tentative redshift z = 0.249, while the elliptical host galaxy has m(host) = 17.7 and M(host) = -24.3. Similar results was obtained from HST images (Scarpa et al. 1999b). Imaging results together with the lack a power law continuum in the optical spectrum (Perlman et al. 1996) strongly suggest it is not a BL Lac source.

A.3. Resolved BL Lacs

1ES 0033+595: The HST observations of this BL Lac at unknown redshift (although a tentative redshift z = 0.086 was derived by Perlman, priv. comm.) have been discussed by Scarpa et al. (1999a). It is a gravitational lens candidate consisting of two objects (A and B; see Scarpa et al. 1999a) with similar R–band brightness and separation of $\sim$1.″6. In addition to R–band images we obtained also data in the U–, B– and V–bands. This allows us to compare colors of the two objects. These turned out to be significantly different with U–B = 0.4 and -0.1, B–V = 1.4 and 1.7, and V–R = 0.9 and 1.9 for A and B, respectively. Due to the bluer color it is likely that the BL Lac is the object B while A is a red galactic star (the source is close to the galactic plane).

The strong color differences strongly argue against the lens hypothesis. The most likely explanation is a chance alignment with a foreground star.

The probable BL Lac in the pair (component B) remained unresolved in the HST snapshot survey (Scarpa et al. 1999b), with an upper limit m(host) $>$20.0. From the analysis of the NOT image we are able to detect an excess of light at radii larger than 2 arcsec corresponding to surface brightness fainter than 24 mag/arcsec^{-2}. If the nebulosity is attributed to the host galaxy this would correspond to an object of 19.0 mag. A caution is however needed for this detection because of the presence of a very bright star in the field that contaminates the background emission.

MS 0205.7+3509: This source, for which WSY96 preferred a disk host galaxy surrounding a significantly de-centered nucleus, was recently studied in detail by us (Falomo et al. 1997). We refuted both the disk model and the gravitational lens interpretation (Stocke et al. 1995), and identified MS 0205.7+3509 as an elliptical host galaxy with no de-centering but with a close companion galaxy.

MS 0317.0+1834: WSY96 could not distinguish between elliptical and disk host for this source, for which they derived M(R) = $-$23.0 and R(e) = 5.1 kpc. After masking out the close companion, we clearly prefer an elliptical host with M(R) = $-$23.7 and R(e) = 4.7 kpc, a somewhat brighter host.

1ES 0347-121: The host galaxy is clearly resolved with the radial profile well described by an elliptical model. We derive for the host M(host) = $-$23.2, identical to that derived by U99b. There is an interacting system of three galaxies located 12 arcsec N of the BL Lac but no signs of a physical connection with the BL Lac are apparent.

1ES 0414+009: This BL Lac was resolved into an elliptical galaxy with M(R) = $-$24.8 by the HST (U99b). It was also studied by Falomo (1996) who derived for the host M(R) = $-$24.3 and R(e) = 5 kpc. We derive for the elliptical host at z = 0.287 M(R) = $-$24.7 and R(e) = 5.8 kpc, in good agreement with the other measurements. This source was also studied by WSY96, who could not distinguish between elliptical and disk morphology. They derived for the host M(R) = $-$24.4 and R(e) = 30.8 kpc. While the host luminosity is in agreement, the scale length from WSY96 is clearly too large. Note that 1ES 0414+009 is the dominant member of a moderately rich cluster at z = 0.287 (Abell class 0; McHardy et al.1992; Falomo et al. 1993).

MS 0419.3+1943: WSY96 derived for the probably elliptical host M(R) = $-$23.5 and R(e) = 22.9 kpc, while U99b derived for the elliptical host M(R) = $-$24.0, and we identify the host as clearly an elliptical with M(R) = $-$24.8 and R(e) = 6.0 kpc.

1ES 0502+675: The HST observations of this BL Lac at z = 0.341 have been discussed by Scarpa et al. (1999a). It is a gravitational lens candidate with a double source of similar magnitude with a separation of only $\sim$0.″3. Scarpa et al. (1999a) found the host galaxy has M(host) = $-$23.9. Using the NOT data we derive for the host galaxy M(host) = $-$24.6. The difference is likely due to the fact that our image is much deeper than the one obtained with HST reaching μ_R = 26.5 at 6 arcsec from the center compared with μ_R = 24 at 2 arcsec from HST image.

MS 0607.9+7108: For this BL Lac at z = 0.267, the morphology of its host galaxy has been controversial, mainly due to the presence of a bright nearby star. WSY96 preferred a disk model (although they could not rule out elliptical host) and derived M(R) = $-$24.8 and R(e) = 8.9 kpc, while HST (U99b) indicated an elliptical host with M(host) = $-$24.3. Because of the presence of the close bright star we have first subtracted a scaled PSF from the image removing the contribution from the star and then extracted the brightness profile from the BL lac. After this correction the surrounding nebulosity turned out to be well represented by a an elliptical model similarly to the rest of the objects.

1ES 0806+524: The HST observations of this BL Lac at tentative z = 0.136 (Bade et al. 1998) have been discussed by Scarpa et al. (1999a). Noteworthy is an arc–like structure $\sim$2″ S of the nucleus. Using the NOT data we derive for the host galaxy M(host) = $-$24.2 to be compared with M(host) = $-$23.5 reported by Scarpa et al. (1999a). The difference can be due in part to poor photometry for this target and to the fact that NOT image is much deeper (μ_R = 26.5) than HST image (μ_R = 24.5) and allow us to detect the host up to 15 arcsec from the center.

MS 0922.9+7459: WSY96 derived for the marginally resolved host M(R) = $-$22.6, while we clearly resolve the elliptical host with M(R) = $-$24.7 and R(e) = 9.7 kpc. The large difference is likely attributable to the difference of seeing (0.7 versus 1.3 arcsec) and therefore the ability to distinguish starlight from nuclear source. This high redshift (z = 0.638) source, which lies behind the rich cluster of galaxies Abell 786 (z = 0.124) and may itself be located in a moderately rich cluster (Wurtz et al. 1997), was also resolved by HST (U99b), with M(R) = $-$24.6, in good agreement with our result.

1ES 1011+496: Our derived magnitude for the elliptical host galaxy, M(R) = $-$23.7, is in good agreement with that derived by the HST (U99b), M(R) = $-$23.6. The redshift of this object is uncertain, being based on the possible membership of the BL Lac to the cluster Abell 950 at z=0.20 (Wisniewski et al. 1986). Some galaxies are indeed detected in the field of view.

1ES 1028+511: Our derived magnitude for the elliptical host galaxy, M(R) = −23.2, is significantly fainter than that derived by the HST (U99b), M(R) = −24.1. Again we believe the difference is attributable to different surface brightness limits of the images. Note that a reliable redshift of z = 0.361 based on CaII H&K absorption lines was recently reported by Polomski et al. (1997), which is considerably larger than the z = 0.239 previously used for this target.

1ES 1218+304: This source has a recently determined redshift of z = 0.182 (Bade et al. 1998). WSY96 derived for the host m(R) = 16.6, while we derive m(R) = 17.6. HST derived for the absolute host magnitude M(R) = −23.6, in good agreement with our result, M(R) = −23.8.

MS 1221.8+2452: U99b derived for the host M(R) = −22.5 and R_e = 4.0 kpc, WSY96 derived M(R) = −22.7 and R_e = 2.6 kpc, and Jannuzi et al. (1997) derived M(R) = −22.8 and R_e = 3.2 kpc. We derive in this study M(R) = −22.7 and R_e = 2.9 kpc, in good agreement with the previous studies.

MS 1229.2+6430: WSY96 derived for the host M(R) = −24.1 and R(e) = 10.6 kpc, and HST (U99b) derived M(R) = −24.1 while we derive M(R) = −24.3 and R(e) = 11.0 kpc, in good agreement with the previous determinations. The elliptical host looks quite symmetric despite the presence of a companion galaxy located 3.4 arcsec SW.

1ES 1255+244: Heidt et al. (1999) derived for the host M(R) = −23.2 and R(e) = 7.2 kpc, and HST (U99b) derived M(R) = −23.3, while we derive M(R) = −23.4 and R(e) = 6.4 kpc, in good agreement with the previous determinations. This BL Lac seems to be embedded in a small cluster of galaxies (Heidt et al. 1999).

MS 1407.9+5954: U99b using HST derived for the host M(R) = −24.8 and R_e = 11.1 kpc, WSY96 derived M(R) = −24.3 and R_e = 9.7 kpc, while Jannuzi et al. (1997) derived M(R) = −24.0 and R_e = 12.2 kpc. We derive in this study M(R) = −23.9 and R_e = 8.0 kpc, in good agreement with the previous studies. This BL Lac is the BCG in a moderately rich cluster (Wurtz et al. 1993, 1997).

MS 1443.5+6349: WSY96 derived for the host which they classified as a probable disk, M(R) = −23.6 and R_e = 11.3 kpc. We clearly classify the host as an elliptical, with M(R) = −23.9 and R_e = 17.2 kpc. This source is surrounded by close companions.

MS 1458.8+2249: WSY96 derived for the host M(R) = −23.6 and R_e = 7.9 kpc, and HST (U99b) derived M(R) = −23.7, while we derive M(R) = −24.3 and R_e = 2.3 kpc, somewhat brighter host. The model fits are hampered by the presence of bright nearby stars.

MS 1757.7+7034: WSY96 derived for the host M(R) = −23.3 and R_e = 6.1 kpc, and HST (U99b) derived M(R) = −23.6, while we derive M(R) = −23.4 and R_e = 2.2 kpc, in good agreement with the previous studies.

1ES 1853+671: Heidt et al. (1999) derived for the host M(R) = −22.9 and R_e = 9.4 kpc, and HST (U99b) derived M(R) = −23.2, while we derive M(R) = −22.7 and R_e = 11.6 kpc, in reasonably good agreement. This BL Lac belongs to a very poor group of galaxies, however, it has a close companion 2″ to the NW (Heidt et al. 1999).

1ES 1959+650: The HST observations of this BL Lac at a tentative redshift z = 0.048 have been discussed by Scarpa et al. (1999a). It is hosted by a gas–rich elliptical galaxy with a prominent dust lane. They are able to clearly resolve the host galaxy whose luminosity is M(host) = −22.5. This BL Lac was also studied by Heidt et al. (1999), who derived for the host galaxy m(host) = 14.8, M(host) = −23.0 and R_e = 12.5 kpc. We derive for the host galaxy m(host) = 16.1, M(host) = −22.7 and R_e = 5.3 kpc. All these determinations are in good agreement with each other, except for the scale length. Note that the absolute host luminosity is in the faintest end of the distribution for the XBLs, suggesting that its distance could be larger than z = 0.048.

1ES 2037+521: Heidt et al. (1999) derive for the host M(R) = −23.2 and R_e = 12.3 kpc, while we derive M(R) = −23.7 and R_e = 7.8 kpc, in reasonable agreement. HST (U99b) derived m(R) = 16.1, in good agreement with the value found here, m(R) = 16.3. A small companion galaxy is visible 0.6 arcsec away from the nucleus, apparently well inside the host.

MS 2143.4+0704: Kotilainen et al. (1998b) derived for the host M(H) = −25.9 and R_e = 5.5 kpc, while we find in this study M(R) = −23.6 and R_e = 10.9 kpc. The scale length is in reasonable agreement. The color of the host is R–H = 2.3, in agreement with the average found for low redshift BL Lacs, R–H = 2.2±0.5 (Kotilainen et al. 1998b). Urry et al. (1999a) and U99b derived for the host M(R) = −23.7, M(I) = −24.1 and R_e = 8.8 kpc, WSY96 derived M(R) = −23.8 and R_e = 11.6 kpc, while Jannuzi et al. (1997) derived M(R) = −23.3 and R_e = 9,0 kpc, in good agreement with our result, M(R) = −23.6.

1ES 2326+174: Heidt et al. (1999) derive for the host M(R) = −23.4 and R_e = 8.5 kpc, and HST (U99b) derived M(R) = −23.7, while we derive M(R) = −24.2 and R_e = 7.5 kpc, slightly brighter host. Part of the 0.8 mag difference with Heidt et al. is probably due to different extinction and K-correction applied since the difference of observed galaxy mag is just 0.5 mag. Three faint galaxies, possibly companions, are superimposed onto the outer parts of the host at 3–6″ distance from the nucleus (Heidt et al. 1999).

References

Abraham,R.G., McHardy I.M., Crawford C.S., 1991, MNRAS 252, 482

Antonucci R., 1993, ARA&A 31, 473

Antonucci R., Ulvestad J.S., 1985, ApJ 294,158

Bade N., Beckmann V., Douglas N.G., et al., 1998, A&A 334, 459

Bahcall J.N., Kirhakos S., Saxe D.H., Schneider D.P., 1997, ApJ 479, 642

Blandford R.D., Rees M.J., 1978, In: Wolfe A.N. (ed.) Pittsburgh Conference on BL Lac Objects. University of Pittsburgh Press, p. 328

Bressan A., Chiosi C., Fagotto F., 1994, ApJS 94, 63

Browne I.W.A., 1983, MNRAS 204, 23

Browne I.W.A., Marcha M.J.M., 1993, MNRAS 261, 795

Capaccioli M., Caon N., D'Onofrio M., 1992, MNRAS 259, 323

Cassaro P., Stanghellini C., Bondi M., et al., 1999, A&A, in press
Celotti A., Maraschi L., Ghisellini G., Caccianiga A., Maccacaro T., 1993, ApJ 416, 118
Coleman G.D., Wu C.C., Weedman D.W., 1980, ApJS 43, 393
Djorgovski S., Davis M., 1987, ApJ 313, 59
Ellingson E., Yee H.K.C., Green R.F., 1991, ApJ 371, 49
Elvis M., Plummer D., Schachter J., Fabbiano G., 1992, ApJS 80, 257(E92)
Falomo R., Pesce J.E., Treves A., 1993, ApJ 411, L63
Falomo R., Pesce J.E., Treves A., 1995, ApJ 438, L9
Falomo R., 1996, MNRAS 283, 241
Falomo R., Kotilainen J., Pursimo T., et al., 1997, A&A 321, 374
Fanaroff B., Riley J.M., 1974, MNRAS 167, 31P
Fukugita M., Shimasaku K., Ichikawa T., 1995, PASP 107, 9Q45
Gioia I.M., Maccacaro T., Schild R.E., et al., 1990, ApJS 72, 567
Govoni F., Falomo R., Fasano G., Scarpa R., 1999, A&A in press
Heckman T.M., 1990, In: Sulentic J.W., Keel W.C., Telesco C.M. (eds.) Paired and Interacting Galaxies. NASA Conf. Publ. 3098, p. 359
Heidt J., Nilsson K., Fried J.W., Takalo L.O., Sillanpaa A., 1999, A&A in press
Heidt J., Nilsson K., Sillanpaa A., Takalo L.O., Pursimo T., 1999, A&A 341, 683
Hoessel J.G., Gunn J.E., Thuan T.X., 1980, ApJ 241, 486
Hutchings J.B., Neff S.G., 1992, AJ 104, 1
Hutchings J.B., Holtzman J., Sparks W.B., et al., 1994, ApJ 429, L1
Jannuzi B.T., Yanny B., Impey C., 1997, ApJ 491, 146
Kollgaard R.I., Wardle J.F.C., Roberts D.H., Gabuzda D.C., 1992, AJ 104, 1687
Kotilainen J.K., Falomo R., Scarpa R., 1998a, A&A 332, 503
Kotilainen J.K., Falomo R., Scarpa R., 1998b, A&A 336, 479
Lamer G., Newsam A.M., McHardy I.M., 1999, MNRAS in press
Lamer G., McHardy I.M., Newsam A.M., 1999, In: Takalo L.O., Sillanpää A. (eds.) BL Lac Phenomenon. ASP Conf. Ser. 159, 381
Landolt A.U., 1992, AJ 104, 340
Lehnert M.D., Heckman T.M., Chambers K.C., Miley G.K., 1992, ApJ 393, 68
Maccacaro T., Wolter A., McLean B., et al., 1994, Astroph. Lett. Comm. 29, 267
Magorrian J., Tremaine S., Richstone D., et al., 1998, AJ 115, 2285
McHardy I.M., Abraham R.G., Crawford C.S., et al., 1991, MNRAS 249, 742
McHardy I.M., Luppino G.A., George I.M., Abraham R.J., Cooke B.A., 1992, MNRAS 256, 655
McLure R.J., Dunlop J.S., Kukula M.J., et al., 1999, ApJ in press
Mobasher B., Sharples R.M., Ellis R.S., 1993, MNRAS 263, 560
Morris S.L., Stocke J.T., Gioia I.M., et al., 1991, ApJ 380, 49 (M91)
Murphy D.W., Browne W.A., Perley R.A., 1993, MNRAS 264, 298
Ostriker J.P., Vietri M., 1990, Nat 344, 45
Owen F.N., Laing R.A., 1989, MNRAS 238, 357
Owen F.N., Ledlow M.J., Keel W.C., 1996, AJ 111, 53
Padovani P., 1992, MNRAS 257, 404
Padovani P., Urry C.M., 1990, ApJ 356, 75
Padovani P., Giommi P., 1995, MNRAS 277, 1477
Perlman E.S., Stocke J.T., 1993, ApJ 406, 430
Perlman E.S., Stocke J.T., Schachter J.F., et al., 1996, ApJS 104, 251 (P96)
Pesce J.E., Falomo R., Treves A., 1995, AJ 110, 1554
Polomski E., Vennes S., Thorstensen J.P., Mathioudakis M., Falco E.E., 1997, ApJ 486, 179
Rönnback J., van Groningen E., Wanders I., Örndahl E., 1996, MNRAS 283, 282
Scarpa R., Urry C.M., Falomo R., et al., 1999a, ApJ 521, 134
Scarpa R., et al., 1999b, ApJS in press
Shull,J.M., Van Steenberg M.E., 1985, ApJ 294, 599
Stanghellini C., Dallacasa D., Bondi M., Della Ceca R., 1997, A&A 325, 911
Stark A.A., Gammie C.F., Wilson R.W., et al., 1992, ApJS 79, 77
Stocke J.T., Morris S.L., Gioia I.M., et al., 1991, ApJS 76, 813
Stocke J.T., Wurtz R.E., Wang Q.D., Elston R., Januzzi B.T., 1992, ApJ 400, L17
Stocke J.T., Wurtz R.E., Perlman E.S., 1995, ApJ 454, 55
Thuan T.X., Romanishin W., 1981, ApJ 248, 439
Urry C.M., Padovani P., 1995, PASP 107, 803
Urry C.M., Falomo R., Scarpa R., et al., 1999a, ApJ 512, 88
Urry, et al., 1999b, ApJ in press (U99b)
Wisniewski W.Z., Sitko M.L., Sitko A.K., 1986, MNRAS 219, 299
Wardle J.F.C., Moore R.L., Angel J.R.P., 1984, ApJ 279, 93
Wurtz R., Ellingson E., Stocke J.T., Yee H.K.C., 1993, AJ 106, 869
Wurtz R., Stocke J.T., Yee H.K.C., 1996, ApJS 103, 109 (WSY96)
Wurtz R., Stocke J.T., Ellingson E., Yee H.K.C., 1997, ApJ 480, 547